DOI:
10.1161/CIRCULATIONAHA.119.042336

Document Version
Peer reviewed version

S-nitrosylation of muscle LIM protein facilitates myocardial hypertrophy through toll-like receptor 3-mediated receptor-interacting protein kinase 3 and NLRP3 inflammasome activation

Running title: S-nitrosylated MLP modulates myocardial hypertrophy

Xin Tang[1], PhD, *et al.*

The full author list is available on page 27.

[#] **Corresponding author.**

[#] Yong Ji, MD, PhD, Key Laboratory of Cardiovascular and Cerebrovascular Medicine, Key Laboratory of Targeted Intervention of Cardiovascular Disease, Collaborative Innovation Center for Cardiovascular Disease Translational Medicine, State Key Laboratory of Reproductive Medicine, Nanjing Medical University, 101 Longmian Avenue, Jiangning District, Nanjing, 211166, Jiangsu, China. Tel: +86 25 8686 8469; Fax: +86 25 8686 8467; E-mail: yongji@njmu.edu.cn.

[#] Yi Han, MD, PhD, Department of Geriatrics, First Affiliated Hospital of Nanjing Medical University, 300 Guangzhou Road, Nanjing, Jiangsu, China. E-mail: hanyi@jsph.org.cn.

[#] Liping Xie, MD, PhD , Key Laboratory of Cardiovascular and Cerebrovascular Medicine, Key Laboratory of Targeted Intervention of Cardiovascular Disease, Collaborative Innovation Center for Cardiovascular Disease Translational Medicine, Nanjing Medical University, 101 Longmian Avenue, Jiangning District, Nanjing, 211166, Jiangsu, China. E-mail: lipingxie@njmu.edu.cn.

Abstract

Background: S-nitrosylation (SNO), a prototypic redox-based posttranslational modification, is involved in the pathogenesis of cardiovascular disease. The aim of this study was to determine the role of S-nitrosylation of muscle LIM protein (MLP) in myocardial hypertrophy, as well as the mechanism by which SNO-MLP modulates hypertrophic growth in response to pressure overload.

Methods: Myocardial samples from patients and animal models exhibiting myocardial hypertrophy were examined for SNO-MLP level using biotin-switch methods. S-nitrosylation sites were further identified through liquid chromatography-tandem mass spectrometry (LC-MS/MS). Denitrosylation of MLP by the mutation of nitrosylation sites or overexpression of S-nitrosoglutathione reductase (GSNOR) was used to analyze the contribution of SNO-MLP in myocardial hypertrophy. Downstream effectors of SNO-MLP were screened through mass spectrometry (MS) and confirmed by co-immunoprecipitation. Recruitment of toll-like receptor 3 (TLR3) by SNO-MLP in myocardial hypertrophy was examined in TLR3 small interfering RNA (siRNA)-transfected neonatal rat cardiomyocytes (NRCMs) and in TLR3 knockout mouse model.

Results: SNO-MLP level was significantly higher in hypertrophic myocardium from patients and in spontaneously hypertensive rats and mice subjected to transverse aortic constriction (TAC). The level of SNO-MLP also increased in angiotensin II (Ang II) or phenylephrine (PE)-treated NRCMs. S-nitrosylated site of MLP at cysteine (Cys) 79 was identified by LC-MS/MS and further confirmed in NRCMs. Mutation of Cys79 significantly

reduced hypertrophic growth in Ang II or PE-treated NRCMs and TAC mice. Reducing MLP S-nitrosylation level by overexpression of S-nitrosoglutathione reductase greatly attenuated myocardial hypertrophy. Mechanistically, MLP S-nitrosylation stimulated TLR3 binding to MLP in response to hypertrophic stimuli, and disrupting this interaction by downregulating TLR3 attenuated myocardial hypertrophy. SNO-MLP also increased the complex formation between TLR3 and receptor-interacting protein kinase 3 (RIP3). This interaction in turn induced NOD-like receptor pyrin domain containing 3 (NLRP3) inflammasome activation, thereby promoting the development of myocardial hypertrophy. **Conclusions:** Our findings revealed a key role of SNO-MLP in myocardial hypertrophy and demonstrated TLR3-mediated RIP3 and NLRP3 inflammasome activation as the downstream signaling pathway, which may represent a novel therapeutic target for myocardial hypertrophy and heart failure.

Keywords: myocardial hypertrophy; S-nitrosylation; MLP; TLR3.

Clinical Perspective

What is new?

- We identified a new S-nitrosylated protein SNO-MLP in myocardial hypertrophy.
- We showed that SNO-MLP contributes to myocardial hypertrophy through TLR3/RIP3 and NLRP3 inflammasome pathway.
- We reported that the deficiency of S-nitrosylated MLP-governed TLR3 alleviates pathological myocardial hypertrophy.

What are the clinical implications?

- Pathological myocardial hypertrophy occurs in the various cardiovascular diseases, but to date, no therapies are available to arrest specifically the disease progression.
- Therapeutic intervention for S-nitrosylation of MLP may be more effective in attenuating myocardial hypertrophy.
- The cysteine 79 of MLP and TLR3 as downstream effector of SNO-MLP represent putative novel therapeutic targets in myocardial hypertrophy and pathological remodeling.

Non-standard Abbreviations and Acronyms

SNO: S-nitrosylation

MLP: muscle lim protein

TLR3: Toll-like receptor 3

GSNOR: S-nitrosoglutathione reductase

NRCMs: neonatal rat cardiomyocytes

TAC: transverse aortic constriction ()

Ang II: angiotensin II

PE: phenylephrine

RIP3: receptor-interacting protein kinase 3

NLRP3: NOD-like receptor pyrin domain containing 3

IL-1β: interleukin-1β

Introduction

Globally, there is a continuous increase in morbidity and mortality rates resulting from cardiovascular disease.[1] Myocardial hypertrophy, occurring in hypertension and aortic stenosis, and the progression of stress-induced heart failure represent an independent risk factor for cardiac mortality;[2] however, the underlying mechanisms of myocardial hypertrophy remain poorly defined, and treatment strategies specific to the pathological hypertrophy process have not been developed.

Muscle LIM protein (MLP), belonging to LIM-only domain family, is located in the skeletal muscle and the myocardium.[3] MLP has been widely reported as a scaffold

protein, binding to other proteins through two zinc finger structure domains (LIM domains).[4] The LIM domain may serve as a protein-binding interface.[5] In cardiac myocytes, MLP is mainly located on the Z-lines of myofibrils and it interacts with many Z-line proteins, including T-cap/telethonin,[6] calcineurin,[7] histone deacetylase 4 (HDAC4),[8] and α-actinin.[9] Studies have shown that MLP plays central roles in the pathogenesis of myogenic differentiation, hypertrophy, and dilated cardiomyopathy.[10-12] MLP knockout mice develop heart failure,[13] highlighting a critical role of MLP in cardiac homeostasis. Recent work however reported that the overexpression of MLP did not modulate myocardial hypertrophy and that total expression level of MLP was not altered in the myocardial hypertrophy.[14] This discrepancy may stem from different post-translational modifications (PTMs) of MLP, rather than total MLP level *per se*, which may play a critical role in myocardial hypertrophic growth.

PTMs represent a vital determining factor in modulating protein functions. Many groups, including ours, have shown that S-nitrosylation contributes to various cardiovascular diseases.[15-18] S-nitrosylation is a reversible, covalent addition of nitric oxide (NO) moiety to cysteine thiols, forming S-nitrosoprotein (SNO-protein), which can regulate protein function and cellular signaling via altering protein conformation, enzymatic activity, protein–protein interactions, and cellular localization.[19] Whether MLP could be S-nitrosylated and whether this specific PTM of MLP might contribute to myocardial hypertrophy, remain an open question.

In the present study, we demonstrated that MLP S-nitrosylation, rather than MLP total protein level, plays a crucial role in myocardial hypertrophy. MLP modification

enhanced MLP binding to toll-like receptor 3 (TLR3) and receptor-interacting protein kinase 3 (RIP3), which stimulate NOD-like receptor pyrin domain containing 3 (NLRP3) inflammasome activation and consequent caspase-1 and interleukin-1β (IL-1β) activation, ultimately promoting myocardial hypertrophy. The activation of inflammasome was identified in cardiomyocytes in pathological conditions. Further, inflammatory response plays an important role in regulating myocardial hypertrophy and heart failure[20-22]. Our data therefore identified S-nitrosylated MLP as a key regulator, which together with TLR3 may serve as putative therapeutic targets in treating pathological myocardial hypertrophy and heart failure.

Methods

The data that support the findings of this study are available from the corresponding author on reasonable request.

Human myocardium samples

Human myocardium samples were collected during cardiac valve replacement surgical procedures and were classified into samples without myocardial hypertrophy and myocardial hypertrophy samples according to prior echocardiographic findings (**Supplemental Table 1**). The study conformed to the principles outlined in the Declaration of Helsinki. The study protocol was approved by the ethics committee of the First Affiliated Hospital of Xiamen University (approval no. KYZ-2014-007). Written informed consent was obtained from all the patients.

Experimental animals

Male spontaneously hypertensive rats (SHRs) and Wistar Kyoto rats of 12 weeks old were obtained from Shanghai SLAC Laboratory Animal Co. Ltd (Shanghai, China). Toll-like receptor 3 (TLR3) knockout (KO) mice were acquired from Dr. Liu Jin and Chen Chan (Department of Anesthesiology and Translational Neuroscience Center, West China Hospital, Sichuan University). The coding region of MLP cDNA was purchased from Hanbio Biotechnology (Shanghai, China). The plasmid construct encoding the complete mouse MLP gene was used to produce AAV9-MLP vectors including AAV9-MLP WT and AAV9-MLP C79A. This recombinant adeno-associated virus 9 (AAV9) was generated in Li Dali laboratory (Shanghai Key Laboratory of Regulatory Biology,

Institute of Biomedical Sciences and School of Life Sciences, East China Normal University). Wild-type male mice of 4 weeks old (C57BL/6J) were intravenously injected with AAV9-GFP, AAV9-MLP WT, and AAV9-MLP C79A (5 X 10^{11} GC/mouse). At 8 weeks after injection, mice were sacrificed and MLP overexpression in the heart was confirmed by western blotting. The AAV9 system was also used in determining the overexpression of S-nitrosoglutathione reductase (GSNOR) in mice hearts. MLP C79A Knock-in mouse line was generated using CRISPR/Cas9 genome editing technology and maintained in C57BL/6 background.

Mouse model of myocardial hypertrophy was generated by thoracic aortic constriction (TAC) surgery on 8 weeks old wild type, TLR3 knockout mice, and AAV9 virus-injected mice. Surgeries were performed according to previously published protocols and sham surgeries were performed in the same way but without constriction of the aorta.[23] Four or eight-week-old male C57BL/6J mice were housed in the Animal Core Facility of Nanjing Medical University with 12-hour light/dark cycles and were fed a standard chow diet. All experiments were conducted randomly, and investigators were blinded to the treatment groups. All animal experiments were approved by the Animal Care and Use Committee of Nanjing Medical University and were conducted in accordance with the National Institutes of Health (NIH) Guide for the Care and Use of Laboratory Animals (approval no. NJMU-1403073/1403076).

Analysis of protein S-nitrosylation by biotin switch assay

A modified biotin switch assay was performed as previously described.[15] Specific nitrosylated proteins were detected using standard immunoblot techniques. MLP

S-nitrosylation was determined by biotin-switch assay using S-nitrosylated protein detection kit (Cayman Chemical, Ann Arbor, USA), according to the manufacturer's instructions. Briefly, free thiols on proteins were blocked using a blocking agent. We lysed and collected cell or tissue proteins with a blocking buffer to block the free thiols and then S-nitrosothiols were reduced to yield free thiols with reducing buffer ascorbic acid (Vitamin C, Vc) and were covalently labeled biotin using labeling buffer. The negative control was not given reducing buffer to reduce nitrosothiols. Subsequent detection using avidin-coupled reagents was used to localize the biotinylated proteins. The biotinylated proteins were incubated overnight at 4°C with Pierce™ NeutrAvidin™ Plus UltraLink™ Resin (ThermoFisher, San Jose, USA) and bound proteins were eluted by boiling at 95 °C with loading buffer and analyzed by SDS-PAGE.

Mass spectrometry determination of S-nitrosylated sites

Liquid chromatography with tandem mass spectrometry (LC-MS/MS) analysis was performed by the Institute of Biophysics, Chinese Academy of Sciences as previously described.[24] Purified heart proteins from spontaneously hypertensive rats (SHRs)/Wistar Kyoto (WKY) rats and transverse aortic constriction (TAC)/Sham mice were blocked using N-ethylmaleimide (NEM) and labeled with biotin-maleimide.[25] Biotinylated proteins were then trypsinized (using a 1: 50 ratio of protein: trypsin) for 16 h and were purified with streptavidin-agarose for LC-MS/MS analysis. Peptides were separated using NanoLC 1D Plus system. Eluting peptide cations were ionized by nanospray and were analyzed using LTQ-Orbitrap XL mass spectrometer (Thermo Scientific). MS/MS spectra were searched against UniProt rat/mouse proteome database using SequestHT.

Statistics

Continuous variables were summarized as mean ± standard error of the mean (SEM). For the comparison of the means between two groups, unpaired 2-sided Student's *t*-test was used when the data showed equal variance test; otherwise, the *t*-test assuming unequal variance was performed. For the comparisons among more than two groups, Brown-Forsythe test was firstly used to evaluate the homogeneity of variance. If the data did pass the equal variance test, one-way ANOVA analysis was used followed by post-hoc analysis using Bonferroni method to adjust for multiple comparisons; otherwise, Welch ANOVA test was performed followed by post-hoc analysis using Tamhane's T2 method. Statistical significance level was set at 0.05 (two-sided) unless otherwise stated. Statistical results and the corresponding methods were presented in the figure legends as well. All the statistical analyses were performed with SPSS Version 25 software (SPSS Inc., Chicago, IL, USA), and the graphs were generated using GraphPad Prism 8 (La Jolla, CA, USA).

Results

S-nitrosylated MLP, but not total MLP, is elevated in human and murine hypertrophic heart

To identify the role of S-nitrosylation in myocardial hypertrophy, a non-biased screening was performed on heart tissues from thoracic aortic constriction (TAC) mice and spontaneously hypertensive rats (SHR) using biotin switch procedures and LC-MS/MS analysis. We identified 126 S-nitrosylated proteins in TAC mouse heart and 79 S-nitrosylated proteins in SHR rat heart (**Supplemental Figure 1**). Comparison between the two datasets identified 32 overlapping targets. MLP is one of the highly S-nitrosylated proteins (**Supplemental Figure 1**).

To determine the role of SNO-MLP in the development of myocardial hypertrophy, we assessed MLP S-nitrosylation level in the myocardial samples from patients undergoing cardiac valve surgery. MLP S-nitrosylation, but not total MLP levels, were significantly higher in hypertrophic heart samples, compared to non-hypertrophic samples (**Supplemental Table 1, Figure 1A**). Consistent with these human data, SNO-MLP, but not total MLP, was increased in the hearts of TAC mice (**Figure 1B**) and SHR rats (**Figure 1C**), compared to corresponding controls. In NRCMs cultures, we treated cells with Ang II (Angiotensin II) or PE (phenylephrine) to mimic hypertrophic conditions and we found higher SNO-MLP levels with unchanged levels of total MLP protein by these hypertrophic stimuli (**Figure 1D-1E**). Thus, these data suggest that SNO-MLP level, rather than total MLP level, is elevated during myocardial hypertrophy.

Cysteine 79 is the S-nitrosylation site of MLP in myocardial hypertrophy

We further identified the specific SNO-site(s) on MLP. MLP has 16 cysteine residues that could potentially be nitrosylated. To explore the specific SNO-site(s) of MLP in myocardial hypertrophy, we employed LC-MS/MS technology. Only Cys79 was identified as modified in the heart tissues from both TAC mice and SHR rats (**Figure 2A, Supplemental Figure 2**). We next transfected Ad-GFP, Ad-MLP WT, and Ad-MLP C79A into NRCMs to detect the level of MLP S-nitrosylation. The transfection efficiency was determined as approximately 80% using adenovirus-encoding GFP (**Supplemental Figure 3**). We found that the expression of exogenous MLP significantly increased while the expression of endogenous MLP was suppressed after transfection of Ad-MLP WT and Ad-MLP C79A, and the level of total SNO-MLP (exogenous and endogenous) was similar in GFP and WT groups (**Figure 2B**). Moreover, Ang II significantly promoted the level of S-nitrosylation of exogenous Flag-MLP, but Cys79 mutation inhibited Ang II-induced S-nitrosylation of exogenous Flag-MLP (**Figure 2B**). These results suggest that Cys79 is the S-nitrosylation site of MLP in myocardial hypertrophy. Subsequently, we administered Ad-GFP, Ad-MLP WT, or Ad-MLP C79A in Ang II or PE-treated NRCMs. Compared to WT-MLP, C79A significantly attenuated the elevation of atrial natriuretic peptide (*Anp*), brain natriuretic peptide (*Bnp*), and β-myosin heavy chain (*β-mhc*) levels and the increase in cell surface area (**Figure 2C-2D, and Supplemental Figure 4**). These data show that Cys79 is the S-nitrosylation site of MLP that may govern cardiac hypertrophic growth.

We next used the siRNA approach to exclude the interference of endogenous MLP. We measured the siRNA efficiency by western blotting, and the silencing efficiency was

up to 75% (**Supplemental Figure 5A**). We designed 3 independent siRNAs against MLP. Both siRNA1 and siRNA2 decreased the level of endogenous MLP, but only siRNA2 (siRNA against 5'UTR of rat *MLP*) decreased endogenous MLP protein level with no effect on exogenous MLP (**Supplemental Figure 5B-5C**). Next, NRCMs were transfected with siRNA2 to silence endogenous MLP and then transfected with Ad-MLP WT or Ad-MLP C79A to overexpress exogenous MLP. RT-PCR analysis showed that we successfully reduced endogenous MLP and overexpressed exogenous MLP (**Supplemental Figure 5D**). More importantly, excluding the interference of endogenous MLP, C79A mutant significantly attenuated the elevation of *Anp*, *Bnp*, and *β-mhc* (**Figure 2E**). These data showed that the overexpression of a non-nitrosylatable form (C79A) of MLP prevents Ang II–induced myocardial hypertrophy and its associated indices, independent of the presence of endogenous MLP.

Inhibition of MLP S-nitrosylation by Cys79 mutation attenuates TAC-induced myocardial hypertrophy

To examine further the cardiac response of SNO-MLP in myocardial hypertrophy *in vivo*, we generated a knock-in mouse in which C79 of MLP was mutated to alanine (MLP C79A) using CRISPR/Cas9 technology (**Supplemental Figure 6A-6B**). MLP C79A mutant and wild type mice of 8 weeks old were subjected to TAC or sham surgery. As shown in **Figure 3A**, TAC surgery significantly increased SNO-MLP in wild-type group; however, in MLP C79A mutant mice, MLP S-nitrosylation was almost disappeared. The impact of MLP C79A mutant on myocardial hypertrophy was assessed by

echocardiography. In TAC-induced hypertrophic hearts, fraction shortening (FS) was lower than in sham group, and C79A mutant alleviated TAC-induced cardiac dysfunction (**Figure 3B**). The results of interventricular septum (IVS) and left ventricular posterior wall thickness (LVPW) also showed that cardiac hypertrophic growth was significantly induced by TAC, and non-nitrosylated MLP group (C79A mutant) alleviated these increases (**Figure 3C-3D, Supplemental Table 2**). We further confirmed that C79A mutant mice attenuated the TAC-induced increase in left ventricular weight/tibia length (LVW/TL) ratio (**Figure 3E**). Hematoxylin-eosin staining measurement of heart cross-sectional area indicated the prevention of TAC-induced hypertrophy of cardiomyocytes by MLP C79A (**Figure 3F**). Thus, these results demonstrate that the inhibition of S-nitrosylation of MLP prevents TAC-induced myocardial hypertrophy and that MLP C79A mutation is protective against pressure overload-induced myocardial hypertrophy.

We also used the exogenous overexpression of adeno-associated virus 9 (AAV9) to detect further the role of SNO-MLP in myocardial hypertrophy. AAV9-GFP, AAV9-MLP WT, and AAV9-MLP C79A were injected intravenously into mice to overexpress Flag-MLP in the heart, respectively (**Supplemental Figure 7A-7B**). The expression of exogenous MLP significantly increased, and endogenous MLP expression was suppressed after transfection of AAV9-MLP WT and AAV9-MLP C79A (**Supplemental Figure 8A**). TAC surgery significantly increased exogenous SNO-Flag-MLP in the AAV9-MLP WT group whilst C79A administration attenuated TAC-induced MLP S-nitrosylation (**Supplemental Figure 8A**).

We next evaluated the impact of inhibiting SNO-MLP at Cys79 on myocardial hypertrophy. Echocardiography indices of IVS and LVPW showed that cardiac hypertrophic growth was significantly induced by TAC, and non-nitrosylated MLP group (C79A mutant) alleviated this increase (**Supplemental Figure 8B-8C, Supplemental Table 3**). We further confirmed that C79A mutant attenuated TAC-induced increase in LVW/TL ratio (**Supplemental Figure 8D**). C79A mutant also alleviated TAC-induced cardiac dysfunction (**Supplemental Figure 8E**). Hematoxylin-eosin staining and wheat germ agglutinin measurement of heart cross-sectional area indicated the prevention of TAC-induced hypertrophy of cardiomyocytes by MLP C79A (**Supplemental Figure 8F**). Consistent with these findings, the induction of *Anp* and *Bnp* by TAC was markedly abrogated by MLP C79A (**Supplemental Figure 9A-9B**). Thus, these results demonstrate that inhibition of S-nitrosylation of MLP prevents pressure overload-induced myocardial hypertrophy.

Denitrosylation of MLP by overexpression of GSNOR mitigates myocardial hypertrophy

To investigate further the role of SNO-MLP in myocardial hypertrophy and the underlying mechanisms, we explored the upstream enzymes that regulate SNO-MLP. NO synthase (NOS) can enhance the level of S-nitrosylation. GSNOR and TRX can denitrosylate S-nitrosylation.[26, 27] Therefore, we examined the expression of these enzymes in primary cells and animal models.

In NRCMs treated with Ang II, SNO-MLP was significantly increased (**Figure 1D**)

whilst NOS and TRX protein levels were not changed (**Supplemental Figure 10A**); however, GSNOR was strongly suppressed (**Figure 4A**). GSNOR was also significantly decreased in the hearts of TAC mice (**Figure 4B**). These data indicate that GSNOR may be the major enzyme of S-nitrosylation, which is involved in myocardial hypertrophy, and decreased expression of GSNOR may promote SNO-MLP. To test this hypothesis, we transfected Ang II or PE-treated NRCMs with Ad-GSNOR. As expected, overexpression of GSNOR significantly suppressed Ang II or PE-induced S-nitrosylation of MLP (**Figure 4C, Supplemental Figure 10B**). The overexpression of GSNOR also prevented Ang II-stimulated cardiomyocyte hypertrophy (**Figures 4D-4E**). To determine whether GSNOR is an upstream S-nitrosylating enzyme of MLP, siRNA against GSNOR was used to transfect NRCMs (**Supplemental Figure 11A**). We then infected the cells with Ad-MLP WT or Ad-MLP C79A to overexpress exogenous MLP. Ang II was administrated to induce hypertrophic growth. RT-PCR results showed that silencing GSNOR expression aggravated cardiomyocyte hypertrophic growth in Ang II induced hypertrophic model, and C79A mutant significantly attenuated this response in GSNOR silencing condition (**Supplemental Figure 11B**). In TAC mice, AAV9-GSNOR and the control virus AAV9-Vector were injected intravenously to overexpress GSNOR in the heart (**Supplemental Figure 12A**). Overexpression of GSNOR prevented the increase in cardiac MLP-SNO (**Supplemental Figure 12B**). Hypertrophic parameters including IVS, LVPW, LVW/TL ratio, and cardiac function parameter of FS was alleviated by GSNOR overexpression, in line with the phenotypes of mice with MLP C79A mutation (**Supplemental Figure 12C-12G, Supplemental Table 4**). Collectively, these data

indicate that decreasing MLP S-nitrosylation by either MLP Cys79 mutation or GSNOR upregulation prevents myocardial hypertrophy.

TLR3 is the downstream effector of SNO-MLP in the regulation of myocardial hypertrophy

To explore the downstream effector(s) of SNO-MLP in regulating myocardial hypertrophy, we further identified proteins that can directly bind SNO-MLP since MLP is a scaffold protein. NRCMs were transfected with WT-MLP and C79A-MLP adenovirus and subsequently treated with Ang II. We conducted a co-immunoprecipitation (co-IP) to enrich MLP protein and performed SDS-PAGE gel for silver staining. Next, we cut off five different strips of the gel to perform MS being unbiased. We identified TLR3 as a new MLP-binding protein (**Figure 5A, Supplemental Figure 13**). To confirm the MS results, co-IP experiments were performed on myocardial samples from patients undergoing cardiac valve surgery. The interaction between MLP and TLR3 was more prominent in hypertrophic hearts than non-hypertrophic samples (**Figure 5B**). In hypertrophic NRCMs and TAC mouse hearts, we found that MLP could indeed bound TLR3, and this binding was enhanced under hypertrophic conditions but attenuated by S-nitrosylation deficiency of MLP (MLP-C79A mutation), at both *in vitro* (**Figure 5C**) and *in vivo* (**Figure 5D**) levels, indicating that SNO modification of MLP can facilitate MLP binding to TLR3.

To examine whether Cys79 is the binding site, we transfected Ad-MLP WT or Ad-MLP C79A into NRCMs to detect the interaction between TLR3 and MLP. The interaction between MLP and TLR3 was not changed (**Supplemental Figure 14**). These findings indicate that Cys79 on MLP may not be the binding site for TLR3 interaction. To

confirm further the protein interaction, we investigated the effects of TLR3 on binding to MLP by an *in vitro* binding assay. We found that the amount of TLR3 bound to MLP significantly increased in GSNO (nitric oxide donor; promoting S-nitrosylation)-treated group compared to non-nitrosylated MLP group (C79A mutant). As expected, no difference between WT and C79A mutant in non-GSNO group was detected for their binding to TLR3 (**Supplemental Figure 15**). Based on these findings, we conclude that SNO-MLP at Cys79 promotes TLR3 binding to MLP.

To evaluate further the role of TLR3 in hypertrophy, we transfected NRCMs with siRNA against TLR3 (**Supplemental Figure 16A**). Silencing TLR3 significantly inhibited Ang II-induced cardiomyocyte hypertrophy, as indicated by fetal gene activation at both protein and mRNA levels (**Figure 6A-6B, Supplemental Figure 16B-16C**). To evaluate the consequences *in vivo*, we used TLR3-KO mice (**Supplemental Figure 16D**) to disrupt fully TLR3 binding to MLP and performed TAC surgery (**Figure 6C**). IVS, LVPW and LVW/TL ratio were all reduced in TLR3-KO-TAC mice compared to WT-TAC controls (**Figure 6D-6F**). And TLR3 deficiency alleviated TAC-induced cardiac dysfunction in TLR3-KO (**Figure 6G, Supplemental Table 5**). Collectively, these results suggest that S-nitrosylation of MLP promotes its binding to TLR3, and knocking down TLR3 to disrupt this interaction prevents pathological myocardial hypertrophy. Thus, TLR3 is a novel contributor to myocardial hypertrophy in response to elevated SNO-MLP and in the presence of hypertrophic stimulus.

SNO-MLP facilitates myocardial hypertrophy through TLR3-mediated RIP3 binding

We next sought to identify the downstream effector(s) of SNO-MLP/TLR3 in the development of myocardial hypertrophy. In previous studies, TLR3 and RIP3 were expressed in cardiomyocytes,[28, 29] and TLR3 has been reported to drive receptor-interacting RIP3 activation via the adaptor protein TIR domain-containing adapter-inducing interferon-β (TRIF) in programmed necrosis.[30]

To determine whether this signaling pathway plays a role in myocardial hypertrophy, interaction of TLR3, RIP3, and TRIF was examined in Ang II-treated NRCMs. Co-IP experiments confirmed that, TLR3 bound MLP together with RIP3 and TRIF. Every protein component in this complex except TRIF was increased in Ang II-induced hypertrophy, compared to control cells (**Figure 7A**). Similar results were obtained in TAC myocardial hypertrophic model (**Figure 7B**). To test whether this complex formation is modulated by SNO-MLP, the co-IP experiments were repeated in Ang II-treated NRCMs transfected with Flag-tagged MLP-WT or MLP-C79A. S-nitrosylation deficient MLP (MLP-C79A mutant), significantly inhibited Ang II-induced complex formation (**Figure 7C**). In TAC mouse hearts, Cys79 mutation also mitigated TAC-induced increase of this complex (**Figure 7D**). These results indicate that the interaction of MLP, TLR3, and RIP3 is enhanced in myocardial hypertrophy and this complex formation is upregulated by increased SNO-MLP level.

NRCMs were transfected with siRNA against 5'UTR of rat MLP and then incubated with Ad-MLP WT or Ad-MLP C79A. In these MLP deficient cells, the increased formation of complex was prevented by MLP-C79A (**Figure 7E**). Considering that TLR3 activates programmed cell death via TRIF and RIP3 interaction, we performed flow cytometry

experiments to assess cell viability. We found that MLP S-nitrosylation did not affect cell survival of Ang II-treated NRCMs incubated with Ad-MLP WT or Ad-MLP C79A (**Supplemental Figure 17**). These data suggest that SNO-MLP enhances the complex formation of MLP, TLR3, and RIP3, but without any significant effect on myocardial cell death during hypertrophic growth. Thus, these findings indicate that MLP, TLR3, and RIP3 interaction is upregulated by SNO-MLP in myocardial hypertrophy.

p65-NLRP3-IL-1β pathway is induced by TLR3 and RIP3 in SNO-MLP-mediated myocardial hypertrophy

To examine further the downstream pathway of TLR3/RIP3 in SNO-MLP-mediated myocardial hypertrophy, we focused on the inflammatory signaling activated by TLR3. We detected several downstream targets of TLR3 in the inflammatory signaling pathway, including p65, TRIF, and IRF3. Here, only change in p65 activity was observed, and not TRIF or IRF3 (**Figure 8A**). Moreover, we found that NLRP3 inflammasome, which was the downstream action of p65, was also activated (**Figure 8A**). We therefore focused on p65-NLRP3-IL1β pathway in SNO-MLP regulated myocardial hypertrophy. The phosphorylation of p65 and NLRP3 was increased in myocardial hypertrophy, which was attenuated by S-nitrosylation deficiency of MLP (MLP-C79A mutation) (**Figure 8A**). To test whether SNO-MLP exaggerates NLRP3-mediated inflammasome formation, confocal microscopy revealed that MLP-C79A significantly attenuated Ang II-induced NLRP3 inflammasome formation (**Figure 8B**).

To confirm the role of NLRP3 in the regulation of myocardial hypertrophy, we used

NLRP3 inhibitor or Si-RNA to suppress NLRP3. MCC950, the NLRP3 inhibitor, significantly reduced Ang II-induced NLRP3 inflammasome formation and myocardial hypertrophy (**Supplemental Figure 18A-18D**). Moreover, NLRP3 knockdown strongly decreased hypertrophic growth in NRCMs, reflecting from the suppression of the Ang II-induced increase in Anp and Bnp expression and myocardial hypertrophy (**Supplemental Figure 19A-19D**). Consistent with these findings, MLP-C79A reduced NLRP3 inflammasome activity as indicated by reduced IL-1β expression, Caspase-1 p20 level and IL-1β secretion *in vitro* (**Supplemental Figure 20A-20B**). Similar results were found in TAC mice (**Figure 8C**). We also detected the activation of IL-1β in the myocardial samples of patients undergoing cardiac valve surgery. Activation of IL-1β was significantly increased in hypertrophic heart samples (**Figure 8D**). Thus, these results demonstrate that S-nitrosylated MLP activates p65-NLRP3-IL-1β axis in myocardial hypertrophy.

Next, to investigate whether RIP3 and p65-NLRP3-IL-1β pathways play a crucial role in regulating myocardial hypertrophy, NRCMs were treated with inhibitors of caspase-1 and RIP3 (VX-765 or GSK'872), respectively. We found that VX-765 and GSK'872 largely attenuated hypertrophy as indicated by *Anp*, *Bnp,* and *β-mhc* mRNA expression (**Supplemental Figure 21A-21C**), implying that RIP3 and p65-NLRP3-IL-1β pathways are both crucial in regulating myocardial hypertrophy. Previous reports suggest that RIP3 is associated with the upstream of NLRP3 inflammasome formation but the regulatory relationship induced by SNO-MLP is not defined[31, 32]. To determine the upstream and downstream relationship between RIP3 and NLRP3 inflammasome in

SNO-MLP-mediated myocardial hypertrophy, NRCMs were treated with GSK'872, a RIP3-inhibitor and NLRP3-IL-1β pathway was examined. RIP3 inhibition with GSK'872 significantly suppressed Ang II-induced IL-1β secretion and expression, as detected by ELISA and western blotting (**Supplemental Figure 21D-21E**). In order to confirm the role of IL-1β in hypertrophy, we performed the experiment that the mice suffered with TAC surgery were treated with IL-1β neutralizing antibodies. Interestingly, IL-1β neutralizing antibodies prevented TAC–induced myocardial hypertrophy and cardiac dysfunction (**Figure 8E-8F, Supplemental Figure 22A-22C, Supplemental Table 6**). These results prove that anti-IL-1β treatment significantly attenuates the TAC-induced hypertrophy, and promotes the cardiac function. Thus, the data presented here suggest that SNO-MLP enhances MLP interaction with TLR3 and RIP3, thence activating p65-NLRP3 inflammasome signaling cascade, thereby working in concert to promote IL-1β secretion and myocardial hypertrophic growth (**Figure 8G**).

Discussion

Our data demonstrate that MLP can be S-nitrosylated and that SNO-MLP is an important positive regulator in myocardial hypertrophy. We have shown that Cys79 is the critical site of MLP for S-nitrosylation in modulating pressure overload-induced myocardial hypertrophy. In addition, our results revealed that MLP interacts with TLR3, a process regulated by MLP S-nitrosylation and we presented convincing evidence for the role of TLR3 in the development of myocardial hypertrophy. These data highlight a novel pathway in the development of myocardial hypertrophy, which may prove amenable to therapeutic intervention.

Although S-nitrosylation of many cardiac proteins has been reported in myocardial remodeling and heart failure,[33] the role of protein S-nitrosylation in modulating myocardial hypertrophy has hitherto been unclear. Our findings revealed the central role of protein S-nitrosylation in hypertrophic signaling in the myocardium. We demonstrated that S-nitrosylation of MLP is increased in human and rodent hypertrophic hearts. MLP has 16 cysteine residues, however only the mutation of Cys79 decreases the level of SNO-MLP and functionally regulates hypertrophy. While there may be multiple cysteine residues in the protein that can be modified, not all of these are involved in pathological cardiac remodeling. These data suggest that the identification of specific sites of SNO modification may be crucial to provide specific therapeutic targets.

To define the role of MLP SNO modification in myocardial hypertrophy, we used different approaches to modulate the level of SNO modification. In addition to mutate SNO-MLP cysteine site, we explored the enzymes that regulate SNO modification. We found that hypertrophic stimuli specifically decreased GSNOR expression.[34, 35] As a denitrosylation protease, GSNOR has been implicated in many biological processes.[35-39] However, the mechanism by which GSNOR is downregulated in myocardial hypertrophy remains unknown. Emerging evidence suggests that NF-κB binds to the promoter of GSNOR and activates the transcription during neuronal differentiation.[40] We speculate that GSNOR may be similarly regulated by certain transcription factors in the presence of hypertrophic stimuli.

Members of TLR family participate in multiple biological processes, such as immune response, differentiation, and cell survival. Recently, TLR4 has been reported to promote

pressure overload-induced myocardial hypertrophy through NF-κB and TLR9.[41, 42] As with TLR4 and TLR9, TLR3 is expressed in cardiomyocytes and it stimulates NF-κB activity, but little is known about its role in the heart. In our study, hypertrophic stimulation promoted TLR3 binding to MLP. Knockdown of TLR3 in response to Ang II decreased the hypertrophy of cardiomyocytes. Similar results were found in TLR3 knockout mice subjected to TAC. Our study therefore provides the first evidence that increased interaction between MLP and TLR3 by hypertrophic stimulation is dependent on S-nitrosylation of MLP and that TLR3 is a positive regulator of myocardial hypertrophy. Meanwhile, S-nitrosylated deficiency for MLP prevented TAC-induced hypertrophy in MLP C79A mutant mice. Interestingly, AAV-MLP C79A also suppressed TAC-induced hypertrophy, suggesting that it could be a novel strategy using AAV-MLP C79A for hypertrophy treatment. In the immune system, dsRNA is the only recognized activator of TLR3.[43] However, in the heart, we found that SNO-MLP activates TLR3 and its downstream effectors in response to hypertrophic stimuli. Previous work has shown that TLR3 or TLR4 directly activates programmed cell death through TRIF and RIP3.[44] Furthermore, TLR3 signaling may lead to distinct cellular outcomes triggered by TRIF via C-terminal RHIM domain interaction with RIP3, followed by activation of NF-κB and initiation of apoptosis via caspase-8.[45] In our study, SNO-MLP enhanced the complex formation of MLP, TLR3, and RIP3, but without any significant effect on myocardial cell death during hypertrophy. Further, RIP3 activated NLRP3-dependent inflammasome and contributed to myocardial hypertrophy. Our data indicate that, in a heart where hypertrophy has not progressed into heart failure, activation of RIP3 does not cause

cardiomyocyte death, but rather stimulates p65-NLRP3 NLRP3-dependent inflammasome pathway in the development of myocardial hypertrophy.[29, 46]

Our data show that in SNO-MLP mediated myocardial hypertrophy, p65-NLRP3 pathway is activated, which induces IL-1β secretion. Recently, a series of clinical trials provided evidence that IL-1β neutralizing antibody therapy is beneficial in cardiovascular diseases.[47, 48] The Canakinumab Anti-inflammatory Thrombosis Outcome Study (CANTOS) showed that post-myocardial infarction subjects treated with IL-1β antibody showed reduced inflammation and cardiovascular event rates.[49] In addition, the administration of IL-1β neutralizing antibody in ApoE$^{-/-}$ mice decreased overall plaque burden.[50] These results confirm IL-1β neutralizing antibody as a promising therapy for ischemic cardiovascular disease. Our results indicate that IL-1β plays an essential role in promoting myocardial hypertrophy, and that IL-1β neutralizing antibody suppresses TAC-induced myocardial hypertrophy, indicating that it is potential for IL-1β neutralizing antibody to treat with myocardial remodeling and heart failure.

In conclusion, our study provides evidence that S-nitrosylation of MLP at Cys79 enhances interaction with TLR3 and RIP3, which activates TLR3/RIP3 signaling to promote myocardial hypertrophy. This work therefore highlights a novel role of MLP S-nitrosylation in myocardial hypertrophy. Targeting SNO-MLP at Cys79 may prove to be a novel strategy in treating pathological myocardial hypertrophy and heart failure in the future.

Acknowledgments

The authors thank Jianming Li, PhD, Animal Core Facility of Nanjing Medical University, China, for generation of the MLP Cys79 mutation mice; Feng Chen, PhD, Yongyue Wei, PhD, Department of Biostatistics, School of Public Health, Nanjing Medical University, China, and Fangrong Yan, PhD, Department of Biostatistics, School of Science, China Pharmaceutical University, China, for the statistical technical assistance.

Sources of funding

This work was supported by grants from the National Key Research and Development Program of China (2019YFA0802704), and the National Natural Science Foundation of China (grant nos. 91639204, 81770287, 81820108002, 81330004, 81670209).

Authors

Xin Tang[1], PhD; Lihong Pan[1], MSc; Shuang Zhao[1], PhD; Feiyue Dai[1], MSc; Menglin Chao[1], PhD; Hong Jiang[1], MSc; Xuesong Li[1], PhD; Zhe Lin[1], PhD; Zhengrong Huang[3], MD, PhD; Guoliang Meng[4], MD, PhD; Chun Wang[5], MD; Chan Chen[6], MD, PhD; Jin Liu[6], MD, PhD; Xin Wang[7], MD, PhD; Albert Ferro[8], PhD, FRCP; Hong Wang[9], MD, PhD; Hongshan Chen[1], MD, PhD; Yuanqing Gao[1], PhD; Qiulun Lu[1], PhD; Liping Xie[1,#], MD, PhD; Yi Han[10,#], MD, PhD; Yong Ji[1,2,#], MD, PhD

Affiliations

[1] Key Laboratory of Cardiovascular and Cerebrovascular Medicine, Key Laboratory of Targeted Intervention of Cardiovascular Disease, Collaborative Innovation Center for

Cardiovascular Disease Translational Medicine, Nanjing Medical University, Nanjing, China;

[2] State Key Laboratory of Reproductive Medicine, Nanjing Medical University, Nanjing, China;

[3] Department of Cardiology, the First Affiliated Hospital of Xiamen University, Xiamen, China;

[4] Nanjing Medical University, Nanjing, China; Department of Pharmacology, School of Pharmacy, Nantong University, Nantong, China;

[5] Department of Geriatrics, Nanjing Drum Tower Hospital, the Affiliated Hospital of Nanjing University Medical School, Nanjing, China;

[6] Department of Anesthesiology and Translational Neuroscience Center, West China Hospital, Sichuan University, Chengdu, China;

[7] Faculty of Biology, Medicine and Health, the University of Manchester, Manchester, UK;

[8] Cardiovascular Clinical Pharmacology, British Heart Foundation Centre of Research Excellence, Cardiovascular Division, King's College London, London, UK;

[9] Department of Pharmacology, Lewis Kats School of Medicine, Temple University, Philadelphia, PA, USA;

[10] Department of Geriatrics, First Affiliated Hospital of Nanjing Medical University, Nanjing, China;

[#] Corresponding author.

Disclosures

None

References

1. Alexander SP, Kelly E, Marrion NV, Peters JA, Faccenda E, Harding SD, Pawson AJ, Sharman JL, Southan C, Buneman OP, Cidlowski JA, Christopoulos A, Davenport AP, Fabbro D, Spedding M, Striessnig J, Davies JA and Collaborators C. THE CONCISE GUIDE TO PHARMACOLOGY 2017/18: Overview. *Br J Pharmacol*. 2017;174 Suppl 1:S1-S16. doi: 10.1111/bph.13882.

2. Shimizu I and Minamino T. Physiological and pathological cardiac hypertrophy. *J Mol Cell Cardiol*. 2016;97:245-262. doi: 10.1016/j.yjmcc.2016.06.001.

3. Buyandelger B, Ng KE, Miocic S, Piotrowska I, Gunkel S, Ku CH and Knoll R. MLP (muscle LIM protein) as a stress sensor in the heart. *Pflugers Arch*. 2011;462:135-142. doi: 10.1007/s00424-011-0961-2.

4. Flick MJ and Konieczny SF. The muscle regulatory and structural protein MLP is a cytoskeletal binding partner of betaI-spectrin. *J Cell Sci*. 2000;113:1553-1564.

5. Zhao JL, Liang SQ, Fu W, Zhu BK, Li SZ, Han H and Qin HY. The LIM domain protein FHL1C interacts with tight junction protein ZO-1 contributing to the epithelial-mesenchymal transition (EMT) of a breast adenocarcinoma cell line. *Gene*. 2014;542:182-189. doi: 10.1016/j.gene.2014.03.036.

6. Knoll R, Hoshijima M, Hoffman HM, Person V, Lorenzen-Schmidt I, Bang ML, Hayashi T, Shiga N, Yasukawa H, Schaper W, McKenna W, Yokoyama M, Schork NJ, Omens JH, McCulloch AD, Kimura A, Gregorio CC, Poller W, Schaper J, Schultheiss HP and Chien KR. The cardiac mechanical stretch sensor machinery involves a Z disc complex that is defective in a subset of human dilated cardiomyopathy. *Cell*. 2002;111:943-955. doi:

10.1016/s0092-8674(02)01226-6.

7. Heineke J, Ruetten H, Willenbockel C, Gross SC, Naguib M, Schaefer A, Kempf T, Hilfiker-Kleiner D, Caroni P, Kraft T, Kaiser RA, Molkentin JD, Drexler H and Wollert KC. Attenuation of cardiac remodeling after myocardial infarction by muscle LIM protein-calcineurin signaling at the sarcomeric Z-disc. *Proc Natl Acad Sci U S A*. 2005;102:1655-1660. doi: 10.1073/pnas.0405488102.

8. Gupta MP, Samant SA, Smith SH and Shroff SG. HDAC4 and PCAF bind to cardiac sarcomeres and play a role in regulating myofilament contractile activity. *J Biol Chem.* 2008;283:10135-10146. doi: 10.1074/jbc.M710277200.

9. Clark KA and Kadrmas JL. Drosophila melanogaster muscle LIM protein and alpha-actinin function together to stabilize muscle cytoarchitecture: a potential role for Mlp84B in actin-crosslinking. *Cytoskeleton (Hoboken)*. 2013;70:304-316. doi: 10.1002/cm.21106.

10. Vafiadaki E, Arvanitis DA and Sanoudou D. Muscle LIM Protein: Master regulator of cardiac and skeletal muscle functions. *Gene*. 2015;566:1-7. doi: 10.1016/j.gene.2015.04.077.

11. Jeong D, Kim JM, Cha H, Oh JG, Park J, Yun SH, Ju ES, Jeon ES, Hajjar RJ and Park WJ. PICOT attenuates cardiac hypertrophy by disrupting calcineurin-NFAT signaling. *Circ Res.* 2008;102:711-719. doi: 10.1161/CIRCRESAHA.107.165985.

12. Lange S, Gehmlich K, Lun AS, Blondelle J, Hooper C, Dalton ND, Alvarez EA, Zhang X, Bang ML, Abassi YA, Dos Remedios CG, Peterson KL, Chen J and Ehler E. MLP and CARP are linked to chronic PKCalpha signalling in dilated cardiomyopathy. *Nat Commun*. 2016;7:12120. doi: 10.1038/ncomms12120.

13. Makarewich CA, Munir AZ, Schiattarella GG, Bezprozvannaya S, Raguimova ON, Cho EE, Vidal AH, Robia SL, Bassel-Duby R and Olson EN. The DWORF micropeptide enhances contractility and prevents heart failure in a mouse model of dilated cardiomyopathy. *eLife*. 2018;7:piie38319. doi: 10.7554/eLife.38319.

14. Kuhn C, Frank D, Dierck F, Oehl U, Krebs J, Will R, Lehmann LH, Backs J, Katus HA and Frey N. Cardiac remodeling is not modulated by overexpression of muscle LIM protein (MLP). *Basic Res Cardiol.* 2012;107:262. doi: 10.1007/s00395-012-0262-8.

15. Wang W, Wang D, Kong C, Li S, Xie L, Lin Z, Zheng Y, Zhou J, Han Y and Ji Y. eNOS S-nitrosylation mediated OxLDL-induced endothelial dysfunction via increasing the interaction of eNOS with betacatenin. *Biochim Biophys Acta Mol Basis Dis*. 2018;1865:1793-1801. doi: 10.1016/j.bbadis.2018.02.009.

16. Zamorano P, Marin N, Cordova F, Aguilar A, Meininger C, Boric MP, Golenhofen N, Contreras JE, Sarmiento J, Duran WN and Sanchez FA. S-nitrosylation of VASP at cysteine 64 mediates the inflammation-stimulated increase in microvascular permeability. *Am J Physiol Heart Circ Physiol.* 2017;313:H66-H71. doi: 10.1152/ajpheart.00135.2017.

17. Hayashi H, Hess DT, Zhang R, Sugi K, Gao H, Tan BL, Bowles DE, Milano CA, Jain MK, Koch WJ and Stamler JS. S-Nitrosylation of beta-Arrestins Biases Receptor Signaling and Confers Ligand Independence. *Mol Cell*. 2018;70:473-487 e6. doi: 10.1016/j.molcel.2018.03.034.

18. Gonzalez DR, Beigi F, Treuer AV and Hare JM. Deficient ryanodine receptor S-nitrosylation increases sarcoplasmic reticulum calcium leak and arrhythmogenesis in cardiomyocytes. *Proc Natl Acad Sci U S A*. 2007;104:20612-20617. doi:

10.1073/pnas.0706796104.

19. Gui L, Zhu J, Lu X, Sims SM, Lu WY, Stathopulos PB and Feng Q. S-Nitrosylation of STIM1 by Neuronal Nitric Oxide Synthase Inhibits Store-Operated Ca(2+) Entry. *J Mol Biol*. 2018;430:1773-1785. doi: 10.1016/j.jmb.2018.04.028.

20. Tripathi D, Biswas B, Manhas A, Singh A, Goyal D, Gaestel M and Jagavelu K. Proinflammatory Effect of Endothelial Microparticles Is Mitochondria Mediated and Modulated Through MAPKAPK2 (MAPK-Activated Protein Kinase 2) Leading to Attenuation of Cardiac Hypertrophy. *Arterioscler Thromb Vasc Biol.* 2019;39:1100-1112. doi: 10.1161/ATVBAHA.119.312533.

21. Zhang Y, Huang Z and Li H. Insights into innate immune signalling in controlling cardiac remodelling. *Cardiovasc Res.* 2017;113:1538-1550. doi: 10.1093/cvr/cvx130.

22. Martini E, Kunderfranco P, Peano C, Carullo P, Cremonesi M, Schorn T, Carriero R, Termanini A, Colombo FS, Jachetti E, Panico C, Faggian G, Fumero A, Torracca L, Molgora M, Cibella J, Pagiatakis C, Brummelman J, Alvisi G, Mazza EMC, Colombo MP, Lugli E, Condorelli G and Kallikourdis M. Single Cell Sequencing of Mouse Heart Immune Infiltrate in Pressure Overload-Driven Heart Failure Reveals Extent of Immune Activation. *Circulation*. 2019;140:2089-2107. doi: 10.1161/CIRCULATIONAHA.119.041694.

23. Meng G, Liu J, Liu S, Song Q, Liu L, Xie L, Han Y and Ji Y. Hydrogen sulfide pretreatment improves mitochondrial function in myocardial hypertrophy via a SIRT3-dependent manner. *Br J Pharmacol*. 2018;175:1126-1145. doi: 10.1111/bph.13861.

24. Yin R, Fang L, Li Y, Xue P, Guan Y, Chang Y, Chen C and Wang N. Pro-inflammatory Macrophages suppress PPARgamma activity in Adipocytes via S-nitrosylation. *Free Radic*

Biol Med. 2015;89:895-905. doi: 10.1016/j.freeradbiomed.2015.10.406.

25. Huang B and Chen C. Detection of protein S-nitrosation using irreversible biotinylation procedures (IBP). *Free Radic Biol Med.* 2010;49:447-456. doi: 10.1016/j.freeradbiomed.2010.05.001.

26. Rizza S and Filomeni G. Chronicles of a reductase: Biochemistry, genetics and physio-pathological role of GSNOR. *Free Radic Biol Med.* 2017;110:19-30. doi: 10.1016/j.freeradbiomed.2017.05.014.

27. Sengupta R and Holmgren A. Thioredoxin and thioredoxin reductase in relation to reversible S-nitrosylation. *Antioxid Redox Signal*. 2013;18:259-269. doi: 10.1089/ars.2012.4716.

28. Chen C, Feng Y, Zou L, Wang L, Chen HH, Cai JY, Xu JM, Sosnovik DE and Chao W. Role of extracellular RNA and TLR3-Trif signaling in myocardial ischemia-reperfusion injury. *J Am Heart Assoc.* 2014;3:e000683. doi: 10.1161/JAHA.113.000683.

29. Zhang T, Zhang Y, Cui M, Jin L, Wang Y, Lv F, Liu Y, Zheng W, Shang H, Zhang J, Zhang M, Wu H, Guo J, Zhang X, Hu X, Cao CM and Xiao RP. CaMKII is a RIP3 substrate mediating ischemia- and oxidative stress-induced myocardial necroptosis. *Nat Med.* 2016;22:175-182. doi: 10.1038/nm.4017.

30. Kaiser WJ, Sridharan H, Huang C, Mandal P, Upton JW, Gough PJ, Sehon CA, Marquis RW, Bertin J and Mocarski ES. Toll-like receptor 3-mediated necrosis via TRIF, RIP3, and MLKL. *J Biol Chem.* 2013;288:31268-31279. doi: 10.1074/jbc.M113.462341.

31. Qin D, Wang X, Li Y, Yang L, Wang R, Peng J, Essandoh K, Mu X, Peng T, Han Q, Yu KJ and Fan GC. MicroRNA-223-5p and -3p Cooperatively Suppress Necroptosis in

Ischemic/Reperfused Hearts. *J Biol Chem.* 2016;291:20247-20259. doi: 10.1074/jbc.M116.732735.

32. Zhang X, Fan C, Zhang H, Zhao Q, Liu Y, Xu C, Xie Q, Wu X, Yu X, Zhang J and Zhang H. MLKL and FADD Are Critical for Suppressing Progressive Lymphoproliferative Disease and Activating the NLRP3 Inflammasome. *Cell Rep*. 2016;16:3247-3259. doi: 10.1016/j.celrep.2016.06.103.

33. Irie T, Sips PY, Kai S, Kida K, Ikeda K, Hirai S, Moazzami K, Jiramongkolchai P, Bloch DB, Doulias PT, Armoundas AA, Kaneki M, Ischiropoulos H, Kranias E, Bloch KD, Stamler JS and Ichinose F. S-Nitrosylation of Calcium-Handling Proteins in Cardiac Adrenergic Signaling and Hypertrophy. *Circ Res.* 2015;117:793-803. doi: 10.1161/CIRCRESAHA.115.307157.

34. Shao Q, Fallica J, Casin KM, Murphy E, Steenbergen C and Kohr MJ. Characterization of the sex-dependent myocardial S-nitrosothiol proteome. *Am J Physiol Heart Circ Physiol.* 2016;310:H505- H515. doi: 10.1152/ajpheart.00681.2015.

35. Casin KM, Fallica J, Mackowski N, Veenema RJ, Chan A, St Paul A, Zhu G, Bedja D, Biswal S and Kohr MJ. S-Nitrosoglutathione Reductase Is Essential for Protecting the Female Heart From Ischemia-Reperfusion Injury. *Circ Res.* 2018;123:1232-1243. doi: 10.1161/CIRCRESAHA.118.313956.

36. Li J, Zhang Y, Zhang Y, Lu S, Miao Y, Yang J, Huang S, Ma X, Han L, Deng J, Fan F, Liu B, Huo Y, Xu Q, Chen C, Wang X and Feng J. GSNOR modulates hyperhomocysteinemia-induced T cell activation and atherosclerosis by switching Akt S-nitrosylation to phosphorylation. *Redox Biol*. 2018;17:386-399. doi: 10.1016/j.redox.2018.04.021.

37. Barnett SD and Buxton ILO. The role of S-nitrosoglutathione reductase (GSNOR) in human disease and therapy. *Crit Rev Biochem Mol Biol*. 2017;52:340-354. doi: 10.1080/10409238.2017.1304353.

38. Hatzistergos KE, Paulino EC, Dulce RA, Takeuchi LM, Bellio MA, Kulandavelu S, Cao Y, Balkan W, Kanashiro-Takeuchi RM and Hare JM. S-Nitrosoglutathione Reductase Deficiency Enhances the Proliferative Expansion of Adult Heart Progenitors and Myocytes Post Myocardial Infarction. *J Am Heart Assoc.* 2015;4: piie001974. doi: 10.1161/JAHA.115.001974.

39. Qian Q, Zhang Z, Orwig A, Chen S, Ding WX, Xu Y, Kunz RC, Lind NRL, Stamler JS and Yang L. S-Nitrosoglutathione Reductase Dysfunction Contributes to Obesity-Associated Hepatic Insulin Resistance via Regulating Autophagy. *Diabetes*. 2018;67:193-207. doi: 10.2337/db17-0223.

40. Wu K, Zhang Y, Wang P, Zhang L, Wang T and Chen C. Activation of GSNOR transcription by NF-kappaB negatively regulates NGF-induced PC12 differentiation. *Free Radic Res*. 2014;48:1011-1017. doi: 10.3109/10715762.2014.906743.

41. Ma D, Zhang J, Zhang Y, Zhang X, Han X, Song T, Zhang Y and Chu L. Inhibition of myocardial hypertrophy by magnesium isoglycyrrhizinate through the TLR4/NF-kappaB signaling pathway in mice. *Int Immunopharmacol*. 2018;55:237-244. doi: 10.1016/j.intimp.2017.12.019.

42. Singh MV and Abboud FM. Toll-like receptors and hypertension. *Am J Physiol Regul Integr Comp Physiol*. 2014;307:R501- R504. doi: 10.1152/ajpregu.00194.2014.

43. Zhan Q, Song R, Li F, Ao L, Zeng Q, Xu D, Fullerton DA and Meng X. Double-stranded

RNA upregulates the expression of inflammatory mediators in human aortic valve cells through the TLR3-TRIF-noncanonical NF-kappaB pathway. *Am J Physiol Cell Physiol*. 2017;312:C407-C417. doi: 10.1152/ajpcell.00230.2016.

44. He S, Liang Y, Shao F and Wang X. Toll-like receptors activate programmed necrosis in macrophages through a receptor-interacting kinase-3-mediated pathway. *Proc Natl Acad Sci U S A*. 2011;108:20054-20059. doi: 10.1073/pnas.1116302108.

45. Kaiser WJ and Offermann MK. Apoptosis induced by the toll-like receptor adaptor TRIF is dependent on its receptor interacting protein homotypic interaction motif. *J Immunol*. 2005;174:4942-4952. doi: 10.4049/jimmunol.174.8.4942.

46. Luedde M, Lutz M, Carter N, Sosna J, Jacoby C, Vucur M, Gautheron J, Roderburg C, Borg N, Reisinger F, Hippe HJ, Linkermann A, Wolf MJ, Rose-John S, Lullmann-Rauch R, Adam D, Flogel U, Heikenwalder M, Luedde T and Frey N. RIP3, a kinase promoting necroptotic cell death, mediates adverse remodelling after myocardial infarction. *Cardiovasc Res.* 2014;103:206-216. doi: 10.1093/cvr/cvu146.

47. Baylis RA, Gomez D, Mallat Z, Pasterkamp G and Owens GK. The CANTOS Trial: One Important Step for Clinical Cardiology but a Giant Leap for Vascular Biology. *Arterioscler Thromb Vasc Biol*. 2017;37:e174-e177. doi: 10.1161/ATVBAHA.117.310097.

48. Hwang MW, Matsumori A, Furukawa Y, Ono K, Okada M, Iwasaki A, Hara M, Miyamoto T, Touma M and Sasayama S. Neutralization of interleukin-1beta in the acute phase of myocardial infarction promotes the progression of left ventricular remodeling. *J Am Coll Cardiol.* 2001;38:1546-1553. doi: 10.1016/s0735-1097(01)01591-1.

49. Ridker PM, Everett BM, Thuren T, MacFadyen JG, Chang WH, Ballantyne C, Fonseca F,

Nicolau J, Koenig W, Anker SD, Kastelein JJP, Cornel JH, Pais P, Pella D, Genest J, Cifkova R, Lorenzatti A, Forster T, Kobalava Z, Vida-Simiti L, Flather M, Shimokawa H, Ogawa H, Dellborg M, Rossi PRF, Troquay RPT, Libby P, Glynn RJ and Group CT. Antiinflammatory Therapy with Canakinumab for Atherosclerotic Disease. *N Engl J Med*. 2017;377:1119-1131. doi: 10.1056/NEJMoa1707914.

50. Gomez D, Baylis RA, Durgin BG, Newman AAC, Alencar GF, Mahan S, St Hilaire C, Muller W, Waisman A, Francis SE, Pinteaux E, Randolph GJ, Gram H and Owens GK. Interleukin-1beta has atheroprotective effects in advanced atherosclerotic lesions of mice. *Nat Med.* 2018;24:1418-1429. doi: 10.1038/s41591-018-0124-5.

Figure legends

Figure 1. S-nitrosylated MLP but not total MLP is significantly higher in myocardial hypertrophy.

A. Representative images for western blotting analysis of SNO-MLP expression in human samples from non-hypertrophic (N = 10) and hypertrophic myocardial tissues (N = 10). Protein expression was quantified and normalized to total MLP or GAPDH.

B. SNO-MLP, total MLP and GAPDH expression in the myocardial tissues of mice at 4 weeks after sham or TAC operation. Protein expression was quantified and normalized to total MLP or GAPDH (N = 6 per group).

C. SNO-MLP, total MLP and GAPDH expression in the myocardial tissues of WKY or SHR rats. Protein expression was quantified and normalized to total MLP or GAPDH (N = 5 per group).

D. Western blotting analysis of S-nitrosylation of MLP expression in Ang II (1 μM) treated NRCMs for 24 h (N = 6 independent experiments).

E. Western blotting analysis of S-nitrosylation of MLP expression in PE (50 μM) treated NRCMs for 24 h (N = 5 independent experiments).

**, $P < 0.01$; ***, $P < 0.001$ (A to C, *t*-test; D and E, *t*-test assuming unequal variance). NS: not significant. SNO-MLP: S-nitrosylation of muscle LIM protein; TAC: transverse aortic constriction; WKY: Wistar Kyoto rat; SHR: spontaneously hypertensive rat; Ang II: Angiotensin II; PE: phenylephrine; NRCMs: neonatal rat cardiomyocytes; -Vc: Without giving reducing buffer ascorbic acid (Vitamin C, Vc) to reduce the nitrosothiols; the negative control of biotin-switch method.

Figure 2. Cysteine 79 is the MLP S-nitrosylation site in myocardial hypertrophy.

A. Representative LC-MS/MS spectra showing target modified peptide fragmentation (Cys79). LC-MS/MS scan of SNO sites of MLP in the myocardial tissues from TAC mice.

B. Western blotting analysis detected S-nitrosylation of endogenous and exogenous SNO-MLP and total MLP levels after Ang II (1 μM, 24 h) incubation in NRCMs transfected with GFP, flag-tagged MLP-WT or C79A mutant for 24 h (N = 5 independent experiments).

C. NRCMs were transfected with Ad-GFP, Ad-MLP-WT or Ad-MLP-C79A and subsequently treated with PBS or Ang II. The levels of *Anp*, *Bnp* and *β-mhc* mRNA expression were detected (N = 5-6 independent experiments).

D. Representative images of NRCMs stained with α-actinin (red). NRCMs were transfected with Ad-GFP, Ad-MLP-WT or Ad-MLP-C79A and subsequently treated with PBS or Ang II for 24 h (N = 3 independent experiments).

E. After knockdown of endogenous MLP, NRCMs were transfected with Ad-MLP-WT or Ad-MLP-C79A and treated with Ang II. The levels of *Anp*, *Bnp* and *β-mhc* mRNA expression were determined by RT-PCR (N = 6 independent experiments).

The comparisons with stars represent statistically significant after adjustment for multiple comparison (*, $P < 0.05$; **, $P < 0.01$; ***, $P < 0.001$; B (top), *t*-test assuming unequal variance; B (bottom), C to E, one-way ANOVA with Bonferroni post-hoc test). ND: not detected; LC-MS/MS: liquid chromatography-tandem mass spectrometry; *Anp*: atrial natriuretic peptide; *Bnp*: brain natriuretic peptide; *β-mhc*: β-myosin heavy chain. Scale bar = 50 μm in D.

Figure 3. A knock-in mutation at Cysteine 79 of MLP attenuates TAC-induced

myocardial hypertrophy

A. Biotin-switch and western blotting analyses of SNO-MLP and total MLP levels following sham or TAC operation in WT- or MLP-C79A-mutation mice.

B. FS values were presented in WT- or MLP-C79A-mutation mice with sham or TAC operation.

C. IVS values were measured after sham or TAC operation in WT- or MLP-C79A-mutation mice.

D. LVPW values were analyzed after sham or TAC operation in WT- or MLP-C79A-mutation mice.

E. LVW/TL ratios were calculated following sham or TAC operation in WT- or MLP-C79A-mutation mice.

F. Histological sections of myocardial tissues from WT- or MLP-C79A-mutation mice with sham or TAC surgery were stained with hematoxylin & eosin (H&E; second and third rows; A-F: N = 7 per group).

The comparisons with stars represent statistically significant after adjustment for multiple comparison (**, $P < 0.01$; ***, $P < 0.001$; A, *t*-test assuming unequal variance; B to F, one-way ANOVA with Bonferroni post-hoc test). ND: not detected; NS: not significant. IVS: interventricular septum; LVPW: left ventricular posterior wall thickness; LVW/TL: left ventricular weight/tibia length; FS: fractional shortening. Scale bar = 200 μm in the second row of F; Scale bar = 100 μm in the third row of F.

Figure 4. Denitrosylation of MLP by GSNOR overexpression mitigates myocardial hypertrophy.

A. Western blotting analysis of GSNOR in PBS- or Ang II-treated NRCMs (N = 6 independent experiments).

B. Western blotting analysis of GSNOR in myocardial tissues from sham or TAC operated mice (N = 6 each group).

C. Representative biotin-switch assay and western blotting analyses of S-nitrosylated MLP in NRCMs overexpressing GSNOR (Ad-GSNOR) or control adenovirus (Ad-PDC) with or without Ang II treatment (N = 6 independent experiments).

D. Representative images of NRCMs stained with α-actinin (red). NRCMs were treated with Ad-GSNOR or Ad-PDC and subsequently incubated with PBS or Ang II (N = 3 independent experiments).

E. NRCMs were treated with Ad-GSNOR or Ad-PDC and subsequently incubated with PBS or Ang II. The mRNA levels of *Anp*, *Bnp* and *β-mhc* expression were detected with RT-PCR (N = 5 independent experiments).

The comparisons with stars represent statistically significant after adjustment for multiple comparison (*, $P < 0.05$; **, $P < 0.01$; ***, $P < 0.001$; A, *t*-test; B, *t*-test assuming unequal variance; C, Welch ANOVA with Tamhane's T2 post-hoc test; D and E, one-way ANOVA with Bonferroni post-hoc test). ND: not detected. Scale bar = 50 μm in D.

Figure 5. TLR3 is downstream of SNO-MLP in the regulation of myocardial hypertrophy.

A. Immunoprecipitation and mass spectrometry assays showing the binding between TLR3 and MLP in NRCMs lysates. MLP-Flag was overexpressed in Ang II-treated cardiomyocytes. The interaction proteins with MLP were immunoprecipitated by Flag antibody.

B. Representative co-immunoprecipitation analysis of MLP and TLR3 in human samples

from non-hypertrophic and hypertrophic hearts (N = 5 per group).

C. Representative co-immunoprecipitation analysis of MLP and TLR3. NRCMs were transfected with Ad-MLP WT or Ad-MLP C79A, and subsequently treated with PBS or Ang II (N = 5 independent experiments).

D. Representative co-immunoprecipitation analysis of MLP and TLR3 in myocardial tissues from mice administrated with AAV9-MLP-WT or AAV9-MLP-C79A and subsequently subjected to sham or TAC operation (N = 4 independent experiments).

The comparisons with stars represent statistically significant after adjustment for multiple comparison (*, $P < 0.05$; B, *t*-test assuming unequal variance; C, one-way ANOVA with Bonferroni post-hoc test; D, Welch ANOVA with Tamhane's T2 post-hoc test). ND: not detected.

Figure 6. Decreasing of TLR3 expression alleviates the myocardial hypertrophy.

A. Pro-ANP, BNP and TLR3 protein levels were detected in TLR3-knockdown NRCMs incubated with PBS or Ang II (N = 7 independent experiments).

B. The mRNA levels of *Anp* and *Bnp* in TLR3-knockdown NRCMs incubated with PBS or Ang II (N = 9 independent experiments).

C. Heart images of *Tlr3*$^{-/-}$ or wild type mice suffered with sham or TAC operation.

D. IVS values were measured in *Tlr3*$^{-/-}$ or wild type mice following sham or TAC operation.

E. LVPW values were analyzed in *Tlr3*$^{-/-}$ or wild type mice suffered with sham or TAC operation.

F. LVW/TL ratios were calculated in *Tlr3*$^{-/-}$ or wild type mice suffered with sham or TAC

operation.

G. FS values were presented in *Tlr3*$^{-/-}$ or wild type mice suffered with sham or TAC operation. *Tlr3*$^{-/-}$ mice with sham group, N = 8; wild type mice with sham group, N = 8; *Tlr3*$^{-/-}$ mice with TAC group, N = 9; wild type mice with TAC group, N = 9. The comparisons with stars represent statistically significant after adjustment for multiple comparison (*, $P < 0.05$; **, $P < 0.01$; ***, $P < 0.001$; A, B, D, E and G, one-way ANOVA with Bonferroni post-hoc test; F, Welch ANOVA with Tamhane's T2 post-hoc test).

Figure 7. S-nitrosylation of MLP enhances complex formation among MLP, TLR3 and RIP3.

A. Co-immunoprecipitation analysis of TLR3, MLP, RIP3 and TRIF in NRCMs treated with PBS or Ang II (N = 5 independent experiments).

B. Co-immunoprecipitation analysis of TLR3, MLP, RIP3 and TRIF in myocardial tissues from sham or TAC operation mice (N = 4 independent experiments).

C. Co-immunoprecipitation analysis of exogenous MLP, TLR3, RIP3 and TRIF in NRCMs infected with Ad-MLP- WT or Ad-MLP-C79A and subsequently treated with PBS or Ang II. (N = 6 independent experiments).

D. Co-immunoprecipitation analysis of exogenous MLP, TLR3, RIP3 and TRIF in myocardial tissues from sham or TAC-operated mice administrated with AAV9-GFP, flag-tagged AAV9-MLP-WT-or AAV9-MLP-C79A (N = 5 independent experiments).

E. NRCMs were transfected with Ad-MLP WT or Ad-MLP C79A after MLP SiRNA transfection and subsequently treated with PBS or Ang II. Representative

co-immunoprecipitation analysis of exogenous MLP, TLR3, RIP3 and TRIF in NRCMs (N = 7 independent experiments).

The comparisons with stars represent statistically significant after adjustment for multiple comparison (*, $P < 0.05$; **, $P < 0.01$; ***, $P < 0.001$; A and B, *t*-test assuming unequal variance; C to E, one-way ANOVA with Bonferroni post-hoc test). NS: not significant. Exo-MLP: exogenous MLP.

Figure 8. p65/NLRP3 is downstream of TLR3 in the regulation of myocardial hypertrophy.

A. NRCMs were transfected with Ad-MLP-WT or Ad-MLP-C79A and subsequently treated with PBS or Ang II. Western blotting assay detected the levels of p-p65, p65, TRIF, p-IRF3, IRF3, NLRP3 and GAPDH expression in NRCMs (N = 3 independent experiments).

B. NRCMs were transfected with Ad-MLP-WT or Ad-MLP-C79A and subsequently treated with PBS or Ang II. Representative images of DAPI (blue), NLRP3 (red) and F-actin (green) in NRCMs were presented.

C. Western blotting analysis of Caspase-1, Caspase-1 p20, pro-IL-1β, IL-1β and GAPDH expression in myocardial tissues from TAC mice administrated with flag-tagged AAV9-MLP-WT or AAV9-MLP-C79A (N = 6 independent experiments).

D. Western blotting analysis of pro-IL-1β, IL-1β and tubulin expression in human samples from non-hypertrophic (N = 5) and hypertrophic hearts (N = 5).

E. IVS values were measured anti-IgG-or anti-IL-1β antibodies treatment in sham or TAC-operated mice.

F. LVPW values were analyzed in anti-IgG-or anti-IL-1β antibodies treatment in sham or TAC-operated mice (E-F: N = 7 per group).

G. Working model of SNO-MLP-induced myocardial hypertrophy through its interaction with TLR3 and RIP3, with subsequent activation of the p65-NLRP3 inflammasome and IL-1β secretion. The comparisons with stars represent statistically significant after adjustment for multiple comparison (*, $P < 0.05$; **, $P < 0.01$; ***, $P < 0.001$; A, C, E and F, one-way ANOVA with Bonferroni post-hoc test; D, *t*-test assuming unequal variance). Scale bar = 20 μm in B.

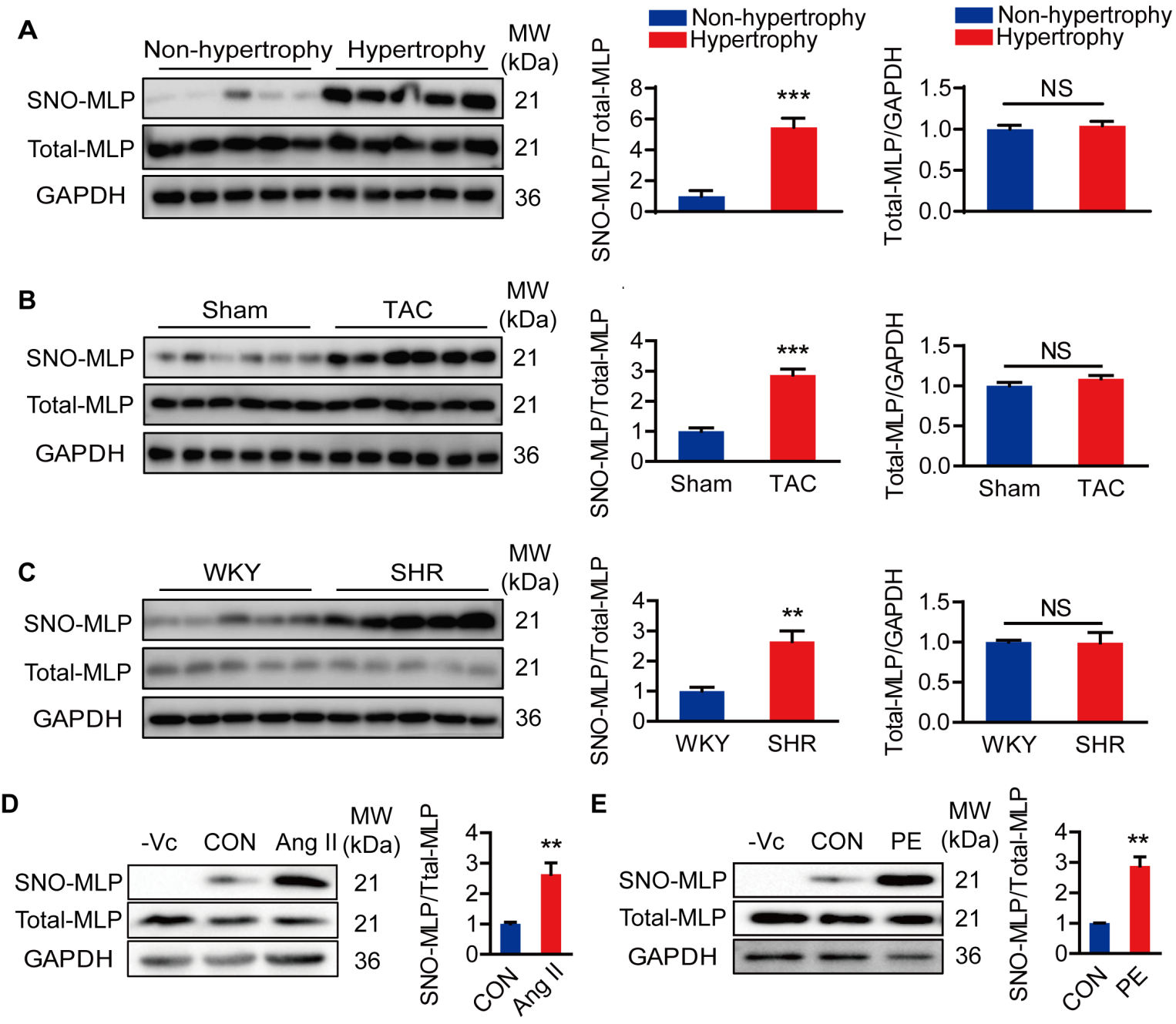
A
Non-hypertrophy
Hypertrophy
MW (kDa)
SNO-MLP
Total-MLP
GAPDH
21
21
36
Non-hypertrophy
Hypertrophy
SNO-MLP/Total-MLP
***
Total-MLP/GAPDH
NS
B
Sham
TAC
MW (kDa)
SNO-MLP
Total-MLP
GAPDH
21
21
36
SNO-MLP/Total-MLP
***
Sham
TAC
Total-MLP/GAPDH
NS
Sham
TAC
C
WKY
SHR
MW (kDa)
SNO-MLP
Total-MLP
GAPDH
21
21
36
SNO-MLP/Total-MLP
**
WKY
SHR
Total-MLP/GAPDH
NS
WKY
SHR
D
-Vc
CON
Ang II
MW (kDa)
SNO-MLP
Total-MLP
GAPDH
21
21
36
SNO-MLP/Ttal-MLP
**
CON
Ang II
E
-Vc
CON
PE
MW (kDa)
SNO-MLP
Total-MLP
GAPDH
21
21
36
SNO-MLP/Total-MLP
**
CON
PE

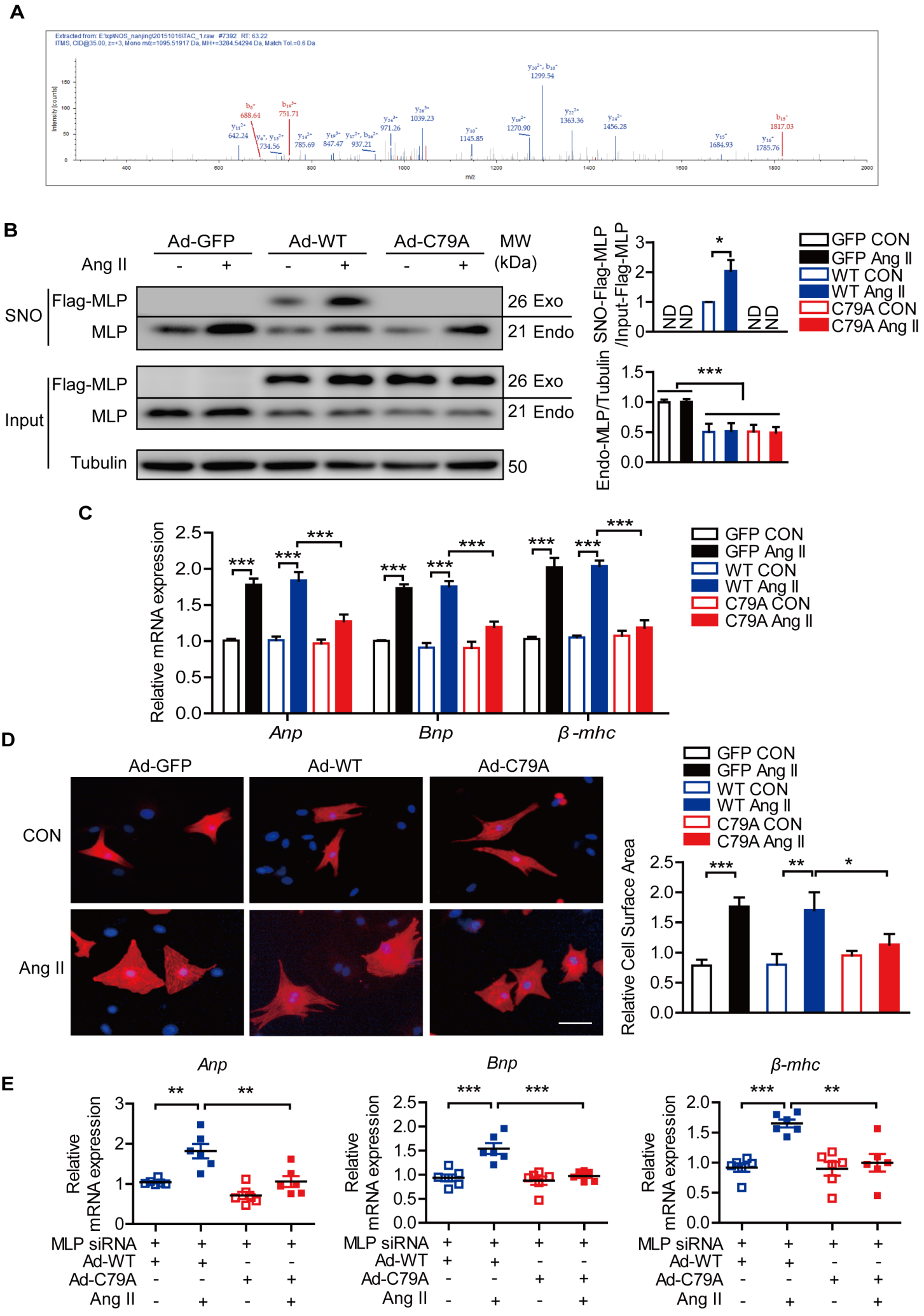
A
B
Ad-GFP
Ad-WT
Ad-C79A
MW (kDa)
Ang II
SNO
Flag-MLP
MLP
Input
Tubulin
26 Exo
21 Endo
50
SNO-Flag-MLP /Input-Flag-MLP
Endo-MLP/Tubulin
GFP CON
GFP Ang II
WT CON
WT Ang II
C79A CON
C79A Ang II
C
Relative mRNA expression
Anp
Bnp
β-mhc
D
CON
Ang II
Relative Cell Surface Area
E
Relative mRNA expression
MLP siRNA
Ad-WT
Ad-C79A
Ang II

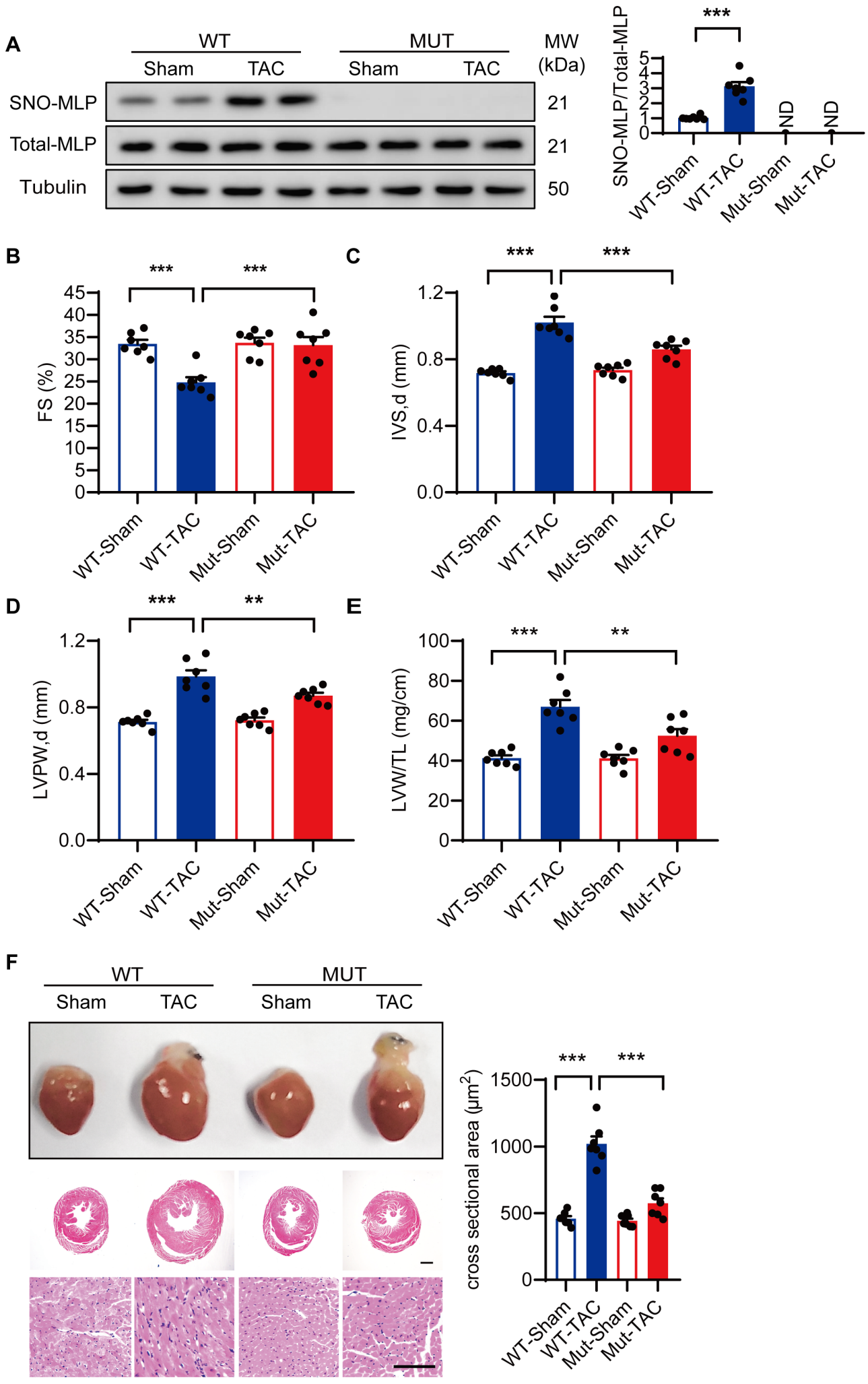
A
WT
MUT
Sham
TAC
Sham
TAC
MW (kDa)
SNO-MLP
Total-MLP
Tubulin
21
21
50
SNO-MLP/Total-MLP
***
ND
ND
WT-Sham
WT-TAC
Mut-Sham
Mut-TAC
B
FS (%)
***
***
C
IVS,d (mm)
***
***
D
LVPW,d (mm)
***
**
E
LVW/TL (mg/cm)
***
**
F
WT
MUT
Sham
TAC
Sham
TAC
cross sectional area (μm²)
***
***

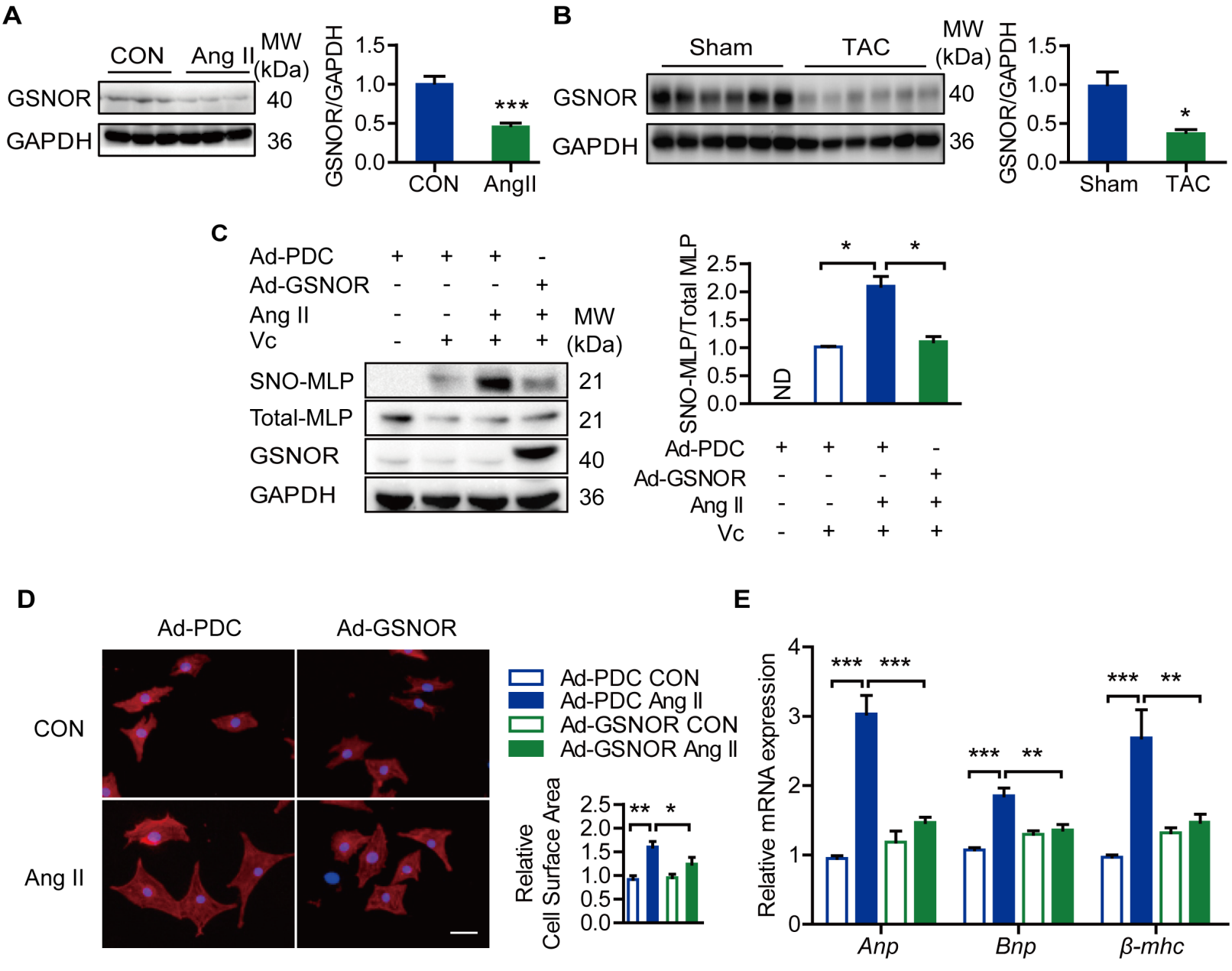
A
CON
Ang II
MW (kDa)
GSNOR
GAPDH
40
36
GSNOR/GAPDH
1.5
1.0
0.5
0.0
***
CON
AngII
B
Sham
TAC
MW (kDa)
GSNOR
GAPDH
40
36
GSNOR/GAPDH
1.5
1.0
0.5
0.0
*
Sham
TAC
C
Ad-PDC + + + -
Ad-GSNOR - - - +
Ang II - - + +
Vc - + + +
MW (kDa)
SNO-MLP
Total-MLP
GSNOR
GAPDH
21
21
40
36
SNO-MLP/Total MLP
2.5
2.0
1.5
1.0
0.5
0.0
ND
*
*
Ad-PDC + + + -
Ad-GSNOR - - - +
Ang II - - + +
Vc - + + +
D
Ad-PDC
Ad-GSNOR
CON
Ang II
Ad-PDC CON
Ad-PDC Ang II
Ad-GSNOR CON
Ad-GSNOR Ang II
Relative Cell Surface Area
2.5
2.0
1.5
1.0
0.5
0.0
**
*
E
Relative mRNA expression
4
3
2
1
0
***
***
***
**
***
**
Anp
Bnp
β-mhc

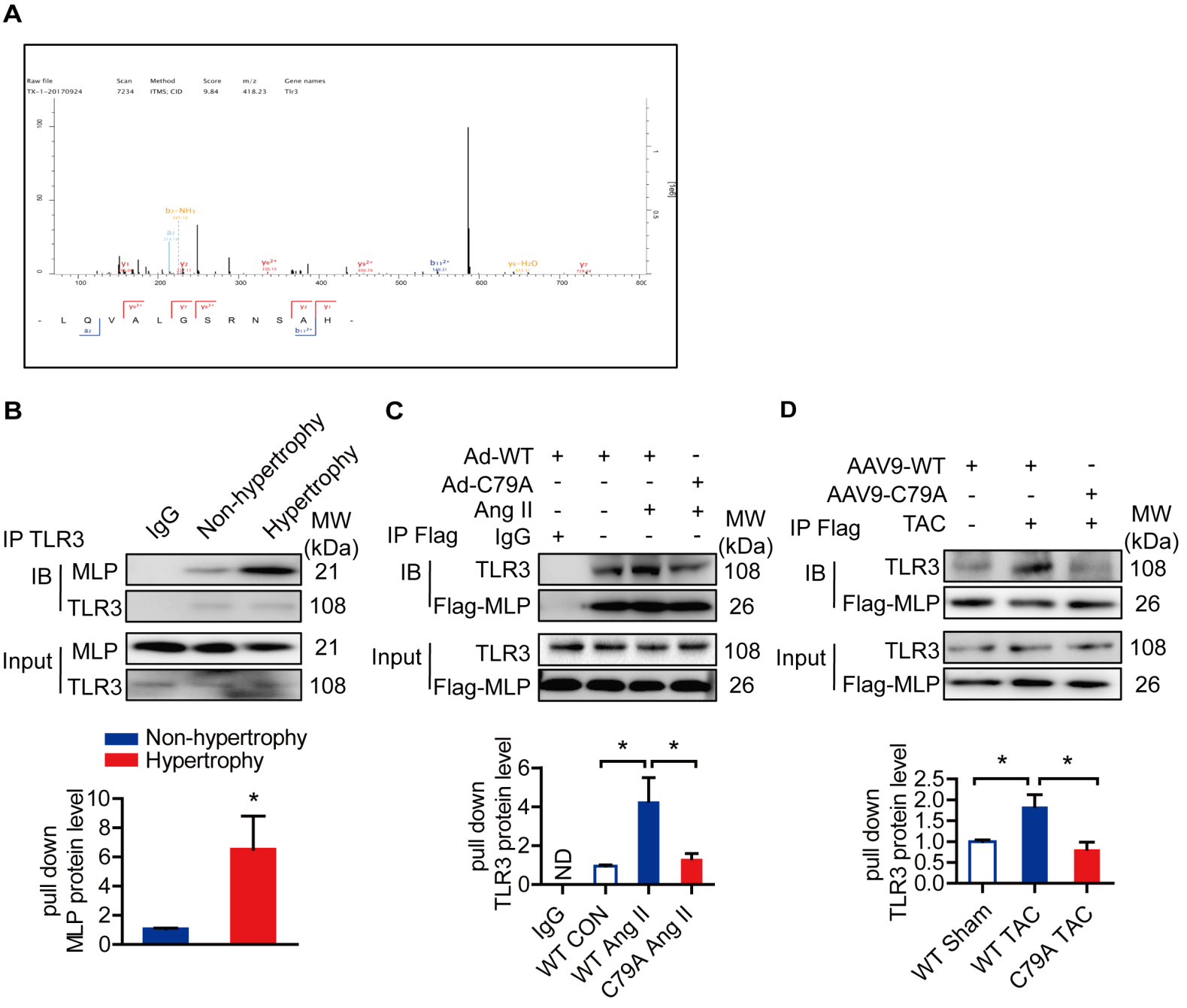
A
Raw file
Scan
Method
Score
m/z
Gene names
TX-1-20170924
7234
ITMS; CID
9.84
418.23
Tlr3
- L Q V A L G S R N S A H -
B
IP TLR3
IgG
Non-hypertrophy
Hypertrophy
MW (kDa)
IB
MLP
21
TLR3
108
Input
MLP
21
TLR3
108
Non-hypertrophy
Hypertrophy
pull down MLP protein level
C
Ad-WT + + + -
Ad-C79A - - - +
Ang II - - + +
IP Flag
IgG + - - -
MW (kDa)
IB
TLR3
108
Flag-MLP
26
Input
TLR3
108
Flag-MLP
26
pull down TLR3 protein level
ND
IgG
WT CON
WT Ang II
C79A Ang II
D
AAV9-WT + + -
AAV9-C79A - - +
IP Flag
TAC - + +
MW (kDa)
IB
TLR3
108
Flag-MLP
26
Input
TLR3
108
Flag-MLP
26
pull down TLR3 protein level
WT Sham
WT TAC
C79A TAC

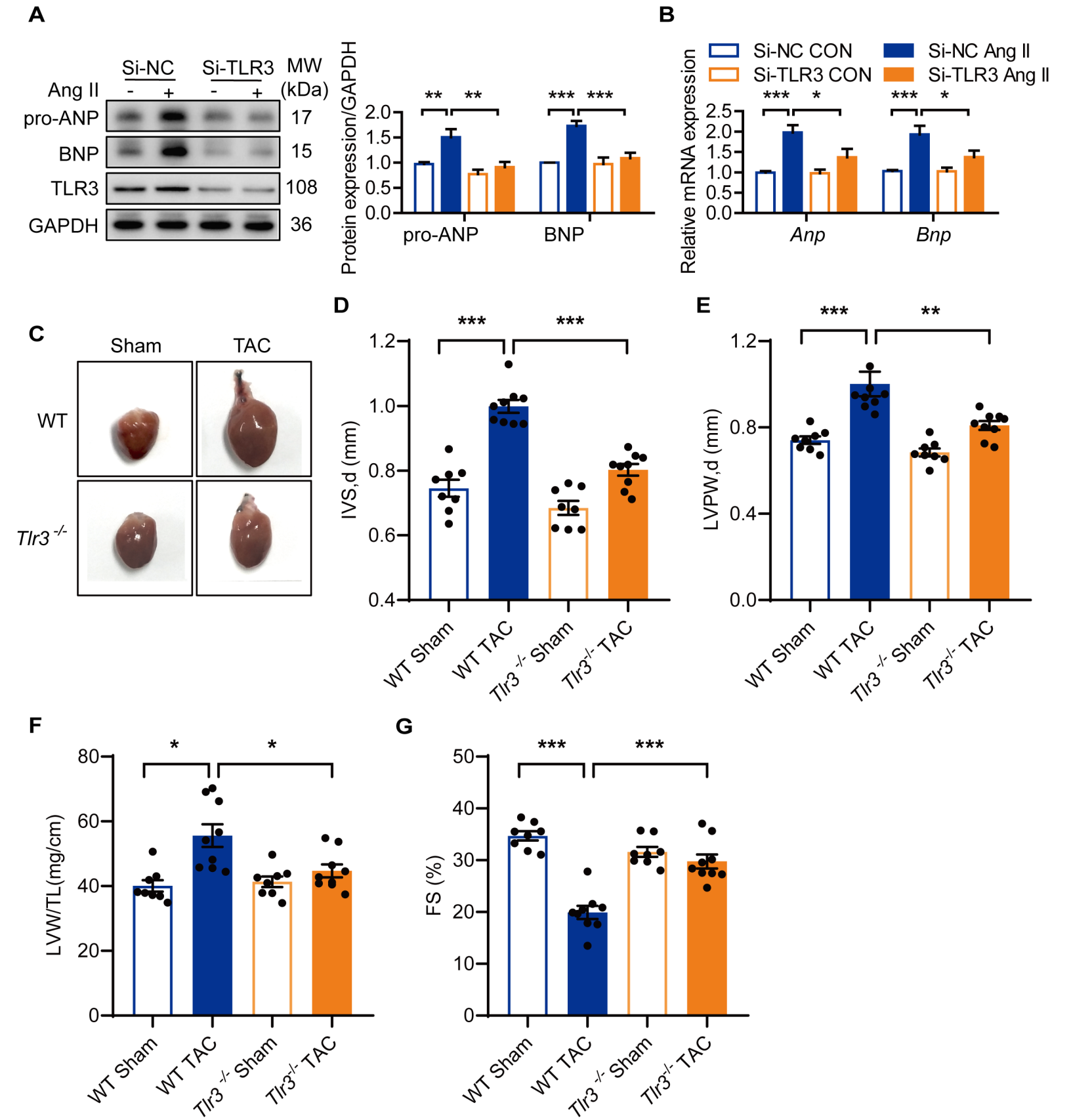
A
Si-NC
Si-TLR3
MW (kDa)
Ang II
- + - +
pro-ANP
BNP
TLR3
GAPDH
17
15
108
36
Protein expression/GAPDH
pro-ANP
BNP
B
Si-NC CON
Si-TLR3 CON
Si-NC Ang II
Si-TLR3 Ang II
Relative mRNA expression
Anp
Bnp
C
Sham
TAC
WT
Tlr3 -/-
D
IVS,d (mm)
E
LVPW,d (mm)
WT Sham
WT TAC
Tlr3 -/- Sham
Tlr3-/- TAC
F
LVW/TL(mg/cm)
G
FS (%)

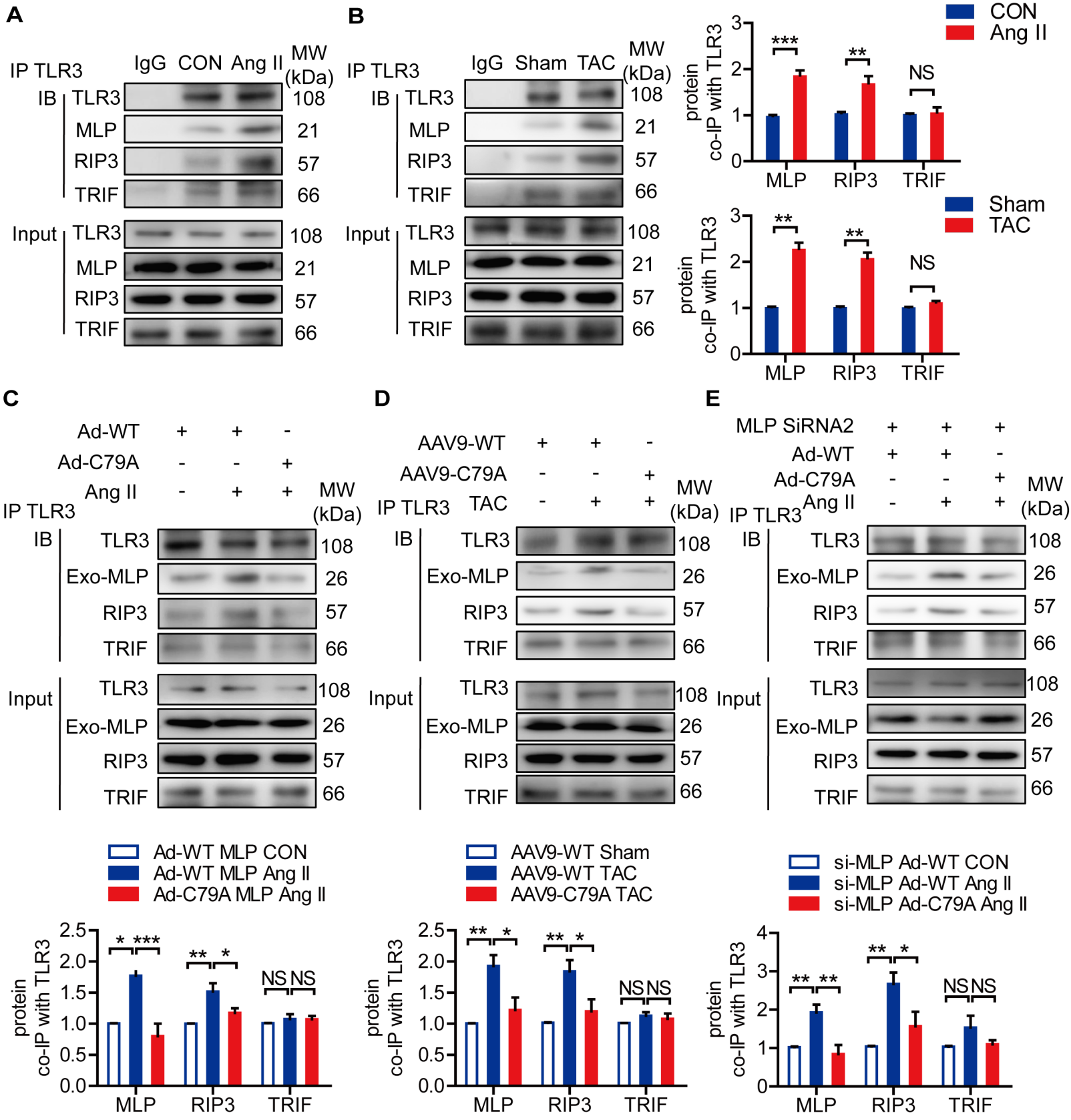
A
IP TLR3
IgG CON Ang II
MW (kDa)
IB
TLR3 108
MLP 21
RIP3 57
TRIF 66
Input
TLR3 108
MLP 21
RIP3 57
TRIF 66
B
IP TLR3
IgG Sham TAC
MW (kDa)
IB
TLR3 108
MLP 21
RIP3 57
TRIF 66
Input
TLR3 108
MLP 21
RIP3 57
TRIF 66
CON
Ang II
protein co-IP with TLR3
***
**
NS
MLP RIP3 TRIF
Sham
TAC
**
**
NS
MLP RIP3 TRIF
C
Ad-WT + + -
Ad-C79A - - +
Ang II - + +
IP TLR3
MW (kDa)
IB
TLR3 108
Exo-MLP 26
RIP3 57
TRIF 66
Input
TLR3 108
Exo-MLP 26
RIP3 57
TRIF 66
Ad-WT MLP CON
Ad-WT MLP Ang II
Ad-C79A MLP Ang II
protein co-IP with TLR3
* ***
** *
NS NS
MLP RIP3 TRIF
D
AAV9-WT + + -
AAV9-C79A - - +
IP TLR3 TAC - + +
MW (kDa)
IB
TLR3 108
Exo-MLP 26
RIP3 57
TRIF 66
Input
TLR3 108
Exo-MLP 26
RIP3 57
TRIF 66
AAV9-WT Sham
AAV9-WT TAC
AAV9-C79A TAC
protein co-IP with TLR3
** *
** *
NS NS
MLP RIP3 TRIF
E
MLP SiRNA2 + + +
Ad-WT + + -
Ad-C79A - - +
IP TLR3 Ang II - + +
MW (kDa)
IB
TLR3 108
Exo-MLP 26
RIP3 57
TRIF 66
Input
TLR3 108
Exo-MLP 26
RIP3 57
TRIF 66
si-MLP Ad-WT CON
si-MLP Ad-WT Ang II
si-MLP Ad-C79A Ang II
protein co-IP with TLR3
** **
** *
NS NS
MLP RIP3 TRIF

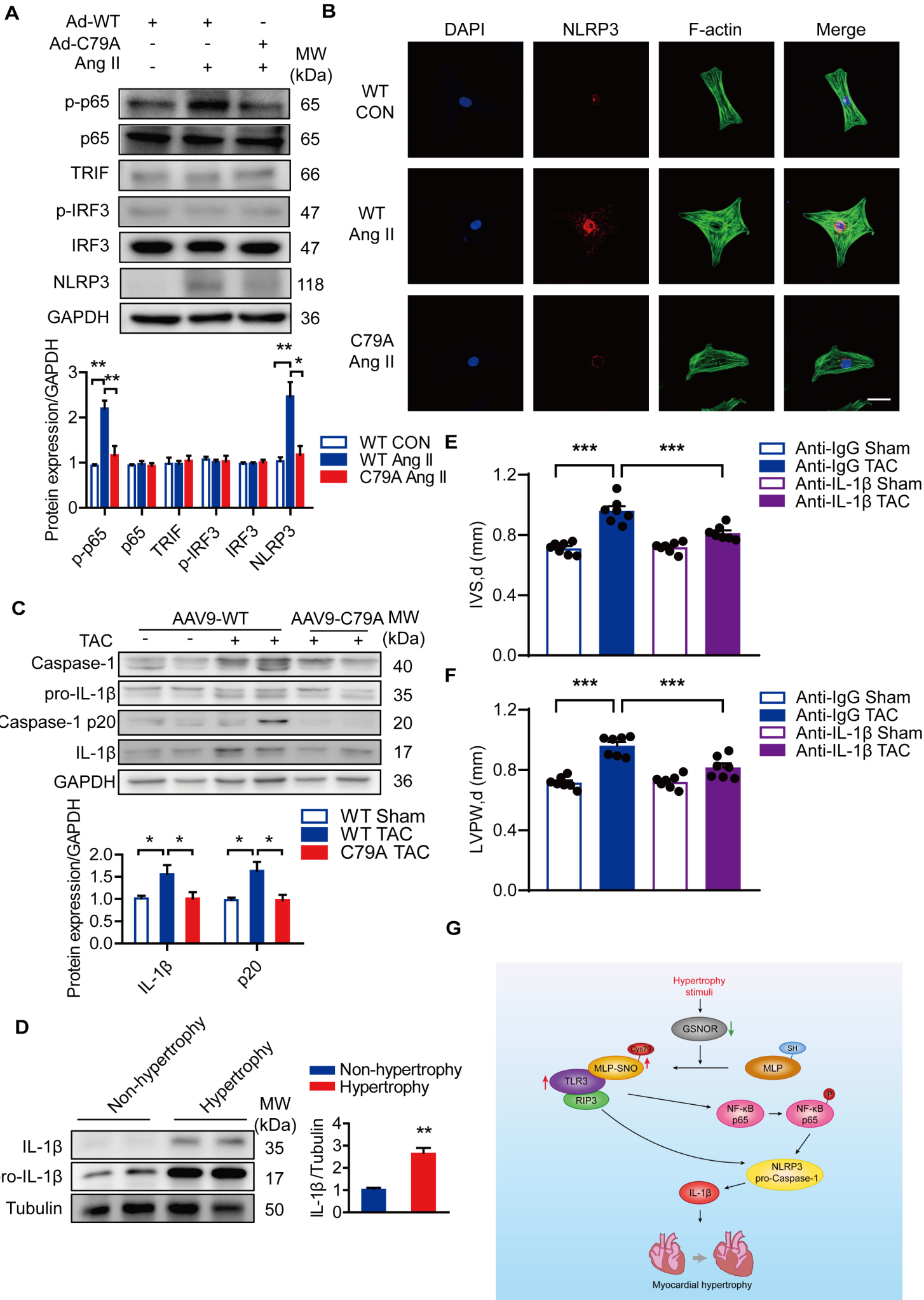
A
Ad-WT
Ad-C79A
Ang II
MW (kDa)
p-p65
p65
TRIF
p-IRF3
IRF3
NLRP3
GAPDH
65
65
66
47
47
118
36
Protein expression/GAPDH
WT CON
WT Ang II
C79A Ang II
B
DAPI
NLRP3
F-actin
Merge
WT CON
WT Ang II
C79A Ang II
C
AAV9-WT
AAV9-C79A
TAC
Caspase-1
pro-IL-1β
Caspase-1 p20
IL-1β
GAPDH
40
35
20
17
36
WT Sham
WT TAC
C79A TAC
IL-1β
p20
D
Non-hypertrophy
Hypertrophy
IL-1β
pro-IL-1β
Tubulin
35
17
50
IL-1β /Tubulin
E
IVS,d (mm)
Anti-IgG Sham
Anti-IgG TAC
Anti-IL-1β Sham
Anti-IL-1β TAC
F
LVPW,d (mm)
G
Hypertrophy stimuli
GSNOR
MLP-SNO
MLP
Cys79
SH
TLR3
RIP3
NF-κB p65
NLRP3 pro-Caspase-1
IL-1β
Myocardial hypertrophy